Faculdade de Engenharia da Universidade do Porto

Combining Antimicrobial Peptides and Graphene in Antimicrobial Catheters

Guilherme Pontes Cardoso de Cavalcanti Mello

Porto, June 2020

Faculdade de Engenharia da Universidade do Porto

Combining Antimicrobial Peptides and Graphene in Antimicrobial Catheters

Guilherme Pontes Cardoso de Cavalcanti Mello

Dissertation carried out under the
Masters in Biomedical Engineering

Supervisor: Dr. Inês Gonçalves (i3S)
Co-supervisor: Dr. Fabíola Costa (i3S)

Porto, June 2020

Abstract

Nowadays, millions of people around the world suffer from end-stage renal disease (ESRD). Most individuals with this medical condition undergo treatments such as hemodialysis (HD) or peritoneal dialysis (PD). Unfortunately, this course of treatment may carry undesired major secondary effects such as the appearance of severe catheter-related infections (CRIs), which represent the main cause of morbidity and second major cause of mortality in these individuals. The exponential development of antibiotic resistance by bacteria and other pathogenic agents is an ever-increasing concern in the scientific and medical community. Therefore, it is important to find new alternative solutions to prevent and treat this kind of infections. Conjugating graphene-based materials (GBMs) with antimicrobial peptides (AMPs) via covalent or non-covalent strategies has been proposed to enhance their antimicrobial properties while also tackling some of their inherent shortcomings at the same time.

The main objective of this work aims at developing novel antimicrobial materials based on the conjugation of AMPs with GBMs. These could afterwards be used as a coating of dialysis catheters, to make them more resistant to bacterial colonization, thus leading to the lower appearance of CRIs in patients. For this purpose, two AMPs (KR-12 and Dhvar5) were selected and their antimicrobial properties studied. Graphene oxide (GO) was the GBM chosen for this work, being its chemical structure and antimicrobial properties investigated. Posteriorly, both GO and AMPs were conjugated via non-covalent (adsorption) and covalent (1-ethyl-3-(3-dimethylaminopropyl)carbodiimide/*N*-hydroxysuccinimide, EDC/NHS coupling chemistry) strategies to evaluate improvements to their inherent properties.

Antimicrobial properties were assessed through minimal inhibitory and bactericidal concentration assays (MIC/MBC) performed with *Staphylococcus epidermidis*, which is one of the bacterial species most commonly associated with bacterial colonization of dialysis catheters. Dhvar5 elicited the lowest MIC and MBC values of 2 μg/mL when compared with the 100 μg/mL obtained by KR-12. The MIC value for GO was 62.5 μg/mL but an MBC value could not be obtained.

Successful production of GO via Modified Hummer's Method (MHM) and conjugation of both AMPs with this material was confirmed via X-ray photoelectron spectroscopy (XPS).

Conjugation of the AMPs with GO did not show signs of improving the original antimicrobial properties of each individual material.

Resumo

Atualmente, milhões de pessoas em todo mundo sofrem de insuficiência renal crónica terminal (IRCT). A maioria dos portadores desta doença tem de iniciar hemodiálise (HD) ou diálise peritoneal (PD), sendo que esta via de tratamentos pode acarretar grandes problemas secundários como o aparecimento de graves infeções relacionadas com o uso de cateteres (IRCs). Este tipo de infeções corresponde à maior causa de morbidade e a segunda maior causa de mortalidade em indivíduos com insuficiência renal crónica terminal. O exponencial desenvolvimento de resistência a antibióticos por parte de bactérias e outros agentes patogénicos é uma crescente preocupação na comunidade médica e científica. Desta forma, é importante que novas alternativas sejam encontradas para a prevenção e tratamento deste tipo de infeções. Materiais derivados de grafeno (MDGs) têm vindo a ser estudados em praticamente todos os campos da ciência devido às duas propriedades estruturais, elétricas, óticas e termais. Mais recentemente, foi descoberto que estes materiais também possuem propriedades antimicrobianas, mostrando que os mesmos podem vir a ter um impacto significativo na área biomédica. Da mesma forma, péptidos antimicrobianos (PAMs) têm vindo a ganhar uma notoriedade crescente como potenciais novos agentes antibióticos devido à sua eficácia e largo espetro de ação contra este tipo de agentes patogénicos. Está provado que a conjugação de MDGs com PAMs através de estratégias que façam uso de ligações covalentes ou não covalentes, pode aumentar as suas capacidades antimicrobianas e retificar algumas das desvantagens inerentes de ambos os materiais.

Desta forma, o presente trabalho tem como objetivo o desenvolvimento de novos materiais antimicrobianos à base da incorporação de PAMs com MDGs, para que estes possam ser utilizados como um revestimento antimicrobiano em cateteres de diálise mais resistentes a colonização por bactérias, levando a um menor aparecimento IRCs. Para este propósito, foram selecionados dois PAMs (KR-12 e Dhvar5) tendo em conta critérios predeterminados e as suas propriedades antimicrobianas foram estudadas. O óxido de grafeno (OG) foi o MDG escolhido para este trabalho. Logo, a sua estrutura química e propriedades antimicrobianas também foram investigadas. Posteriormente, o óxido de grafeno e os péptidos antimicrobianos foram conjugados através de estratégias não covalentes (adsorção) e covalentes (química 1-etil-3-(3-dimetilaminopropil)carbodiimida/N-Hidroxisuccinimida) numa tentativa de melhorar as suas propriedades intrínsecas.

As propriedades antimicrobianas foram avaliadas através de ensaios de concentração inibitória mínima (CIM) e concentração bactericida mínima (CBM) utilizando a Staphylococcus

epidermidis, uma das espécies bacterianas mais associadas com a colonização de cateteres de diálise e subsequente aparecimento de IRCs.

Dhvar5 foi o PAM que alcançou os menores valores de CIM e CBM com 2 μg/mL, quando comparados com os 100 μg/mL obtidos pelo KR-12. O valor de CIM obtido para o OG foi de 62.5 μg/mL, mas o valor de CBM não pode ser obtido.

A produção bem sucedida de OG foi obtida através do método de Hummers modificado (MHM) e conjugação deste material com os PAMs foi confirmada por espectroscopia de fotoeletrões excitados por raios X (XPS).

A conjugação dos PAMs com o OG não mostrou sinais de melhorar as propriedades antimicrobianas originais de cada um dos materiais.

The work described in this thesis was conducted at:

I3S - Instituto de Investigação e Inovação em Saúde / INEB – Instituto de Engenharia Biomédica; Universidade do Porto

The work described in this thesis was financially supported by:

Projects PTDC/CTM-BIO/4033/2014 and PTDC/CTM-COM/32431/2017, and through UID/BIM/04293/2019 funded by national funds through FCT/MCTES (PIDDAC).

Acknowledgements

I would like to express my deepest gratitude to my supervisor, Inês Gonçalves, who invited me to work and welcomed me in her team, giving me the opportunity to conduct this study and collaborate with incredible people. Thank you for always pushing me and giving me invaluable suggestions, as well as being one the most incredibly driven and hard-working people I have ever met. I admire you and I am also inspired by you.

To my co-supervisor, Fabíola Costa, for always being patient with me and helping with whatever I needed. Your deep knowledge about antimicrobial peptides was incredibly valuable to me and your constructive criticism helped me become a better student and researcher. Like Inês, I always fell inspired by your work.

To Cristina Martins and the Bioengineered Surfaces Group, thank you making me feel welcome and appreciated. I have the deepest feeling of gratitude towards you. To my closest friends in the lab, Andreia, Duarte and Patrícia and Sofia for always having a word of encouragement and teaching me all the twists and turns of working in the lab. I cannot thank you enough for your endless patience and generosity. A special thank you to Bruna Costa for sticking with me and giving me orientation in the beginning of my antimicrobial studies, and also Pedro Alves who was always available to help me.

To Daniela Silva, from CEMUP, for all the help and guidance with everything XPS related.

To everyone that works with me in Sushi em Tua Casa, you are the best people to work with and I always feel happy when I am with you.

To all my incredible friends that have been with me for most of my life and also the ones that I have met most recently. Marcelo, Mariana, Pedro Soares, Pedro Ferreira, Rita, Sandra e Sara. There are not words that can express how much I value your friendship. You are one of the main reasons that I was able to get this far. Thank you, my dear friends.

Lastly, a very special and heart-warming thank you to all of my family. I would like to specially thank my mom, who is the strongest person that I have ever met or ever will meet. You are my cornerstone and the person that I always look up to whenever I need strength and inspiration. Thank you for all the support and love that you give me every single day.

Contents

List of Figures

List of Tables

List of Abbreviations

AMP- Antimicrobial peptide
CuAAC- Copper-catalysed alkyne-azide cycloaddition
CFUs – Colony forming units
CKD – Chronic kidney disease
CRIs – Catheter-related infections
dH_2O – Distilled water
EDC - 1-ethyl-3-(3-dimethylaminopropyl)carbodiimide
ESRD – End stage renal disease
FTIR – Fourier transform infrared spectroscopy
G – Graphene
GBM- Graphene-based material
GBP – Graphene-binding peptide
GFR – Glomerular filtration rate
GO – Graphene oxide
HD – Hemodialysis
IN – Indolicidin
MBC – Minimal bactericidal concentration
MHM – Modified Hummer's Method
MIC – Minimal inhibitory concentration
MRSA - Methicillin-resistant *Staphylococcus aureus*
MW – Molecular weight
NHS - *N*-hydroxysuccinimide
NIS - Nisin
PD – Peritoneal dialysis
pDA – Polydopamine
PDNPs - Polydopamine nanoparticles
PEG – Polyethylene glycol
PLL - ε-poly-L-lysine
PU - Polyurethane
rGO – Reduced graphene oxide
TSB – Tryptic soy broth
XPS – X-ray photoelectron spectroscopy

Chapter I: Introduction

1 - Framework

End Stage Renal Disease (ESRD) affects between 0,1-0,2% of the world's population, and two-thirds of the people affected by this disease receive haemodialysis (HD), one quarter perform kidney transplants and approximately one tenth receive peritoneal dialysis (PD) [1, 2].

In 2010, 2.7 to 7.1 million deaths due to ESRD were registered [3]. However, these numbers may be underestimated since kidney disease frequently originates from complex pre-existing medical conditions, being often considered a comorbidity of diabetes and hypertension.

In addition to human loss, ESRD also conveys an immense economic stress to global economies. Even though only 0.03% of the population of developed high-income countries is affected by this disease, almost 5% of their annual health-care budget is spent on ESRD treatments [4]. Considering milder forms of chronic kidney disease (CKD), the total treatment spending is much greater than of the more severe cases of ESRD. Indeed, in 2015, Medicare (a national health insurance program in the United States) spent over 64 billion and 34 billion dollars on CKD and ESRD, respectively [5].Patients with ESRD are very likely to develop catheter-related infections (CRI), a condition that can be defined by the presence of bacteremia originating from central venous catheters and peritoneal dialysis catheters [6, 7]. CRIs caused by antibiotic resistant bacteria are the main cause of morbidity and the second cause of mortality, behind cardiovascular events in ESRD patients undergoing dialysis [8, 9]. Currently available treatments for CRIs usually involve the administration of antibiotics which have been directly linked to the appearance and widespread of antibiotic resistance. Additionally, the administration of high-dose antibiotics can cost patients anywhere between 50$ to 150$ per day [10].

2 - Motivation

The lethality and economical burden associated to CRIs in ESRD patients and the widespread of antibiotic resistance makes this field one of extreme importance, particularly when it comes to the development of novel materials that could prevent or diminish the use of antibiotics. These novel materials could potentially revolutionize the way CRIs are prevented and treated, not only offering a better solution for patients with this type of infections as

opposed to the administration of antibiotics, but also by possibly reducing the economical costs to both hospital and patient.

Graphene-based materials (GBMs) and antimicrobial peptides (AMPs) are two promising candidates for this type of application since both of them possess antimicrobial activity and are less prone to promote antimicrobial resistance. Furthermore, these two materials can be combined via non-covalent and covalent strategies, which have been reported to lead to a synergistic antimicrobial effect against bacteria, while also overcoming some limitations of the materials themselves, such as the susceptibility of AMPs to proteolytic degradation, for example.

3 - Objectives

The main objective of this work is to develop novel biomaterials that can potentially be applicable as an antimicrobial coating on to dialysis catheters, in order to create a medical device capable of preventing infection onset. For that, GBMs and AMPs, both known for having antimicrobial properties, will be combined.

3.1 - Specific objectives

The specific objectives for this work were:

1- Selection of the AMPs;
2- Selection and production of GBM;
3- Evaluation of the antimicrobial activity of the selected AMPs and GBM;
4- Preparation of AMP/GBM conjugates;
5- Chemical characterization of the AMP/GBM conjugates;
6- Evaluation of the antimicrobial properties of AMP/GBM conjugates.

4 – Structure of the Dissertation

The present thesis is organized in five main chapters.

Chapter I contextualizes the dissertation focus, briefly mentioning the problems and motivations that led to the development of this work, as well as, the main objectives that were defined.

Chapter II consists of literature review that introduces this work. This chapter is divided in four main parts. The first one addresses ESRD pathophysiology, epidemiology and and highlighting the burden of CRIs that we are trying to tackle. The second and third groups explore the information regarding GBMs and AMPs and their promising applications in the biomedical field. The last group of this chapter explores the existing strategies (non-covalent and covalent) for combining AMPs with GBMs.

The methodology developed and used, during materials production, characterization and antibacterial effect is presented in Chapter III. The selection of the AMPs was the first step in this study. KR-12 and Dhvar5 were chosen as the AMPs to be studied since they met specific requirements that had been previously defined such as: the bacteria that it targeted, mode of action, spectrum of activity, size and inclusion of aromatic groups. The selection and

subsequent production of GBMs were, as with the selection of the AMPs came next. For this work, graphene oxide (GO) was chosen to be produced and conjugated with the selected AMPs, since it was known that its chemical structure offered more possibilities in terms of conjugation due to the existence of oxygen functional groups. Additionally, stronger bactericidal properties have been associated to oxidized forms of GBMS [11, 12]. Assessment of the antimicrobial properties of the AMPs and GO was performed in order to evaluate their effectiveness against *S. epidermidis* and decide whether or not they were promising candidates to conjugated between themselves.

After careful review of current literature on strategies to conjugate AMPs with GO, we selected two different approaches to accomplish this objective. The first one involved a non-covalent approach by which we could adsorb the selected AMPs to the surface of the GO particles. The second one involved a covalent approach, 1-ethyl-3-(3-dimethylaminopropyl)carbodiimide/N-hydroxysuccinimide (EDC/NHS) coupling chemistry, as this chemistry could theoretically create covalent bonds between the amine groups from the AMPs and the carboxyl groups of the GO. After confirming that the AMPs and GO had been successfully conjugated, it was now time to evaluate the antimicrobial properties of the conjugates against *S. epidermidis* and see if it was possible to obtain a synergistic effect between the two antibacterial agents.

Chapter IV presents the obtained results and further discussion regarding GO, production of AMP/GO conjugates production, AMPs and GO individual and combined antimicrobial properties.

Lastly, Chapter V summarizes the main conclusions of this thesis and suggests future considerations for work that can be done to built upon the obtained results.

Chapter II: Literature Review

1. End Stage Renal Disease

End Stage Renal Disease (ESRD) is an irreversible medical condition that arises from the evolution of Chronic Kidney Disease (CKD) , reaching the point where kidneys are operating at below 15 % of their normal capacity (stage 5) (Table 2.1) [13]. Kidneys work by filtering the blood, removing the waste (from food), drugs and toxic substances, as wells as, excess fluid from the body, maintaining an overall fluid balance. Additionally, they are also responsible for regulating and filtering minerals (magnesium, sodium, potassium, *etc.*) from blood, and are active participants in the creation of important hormones for the erythropoiesis process and blood pressure regulation [14]. Kidney function is best assessed by glomerular filtration rate (GFR), a test that estimates how much blood passes through the glomeruli each minute [15]. It does so by means of a mathematical formula that accounts for parameters such as the person's age, race, gender and serum creatinine levels. Creatinine is a waste product originated from muscle activity, being removed by kidneys, when they are performing well. An increase in creatinine levels indicates that kidney function/GFR is slowing down [15].

Normal kidney function can be impaired due to pre-existing conditions, leading to progressive damage over time, that can be fatal in the absence of adequate treatment. Such conditions include type 1 and 2 diabetes, high blood pressure, glomerulonephritis, polycystic kidney disease, obstruction of the urinary tract by kidney stones and cancers, among others [13].

Table 2.1 - Stages of Chronic Kidney Disease (CKD).

5 Stages of CKD		
	Kidney Function / GFR	**Description**
Stage 1	> 90%	Normal or high function
Stage 2	60 – 89%	Mildly decreased function
Stage 3	30 – 59%	Mild to moderately decreased function
Stage 4	15 – 29%	Severely decrease function
Stage 5 (ESRD)	< 15%	Kidney failure

The lack of function of this vital organ leads to significant modifications in fluid retention, accompanied by disturbances in mineral metabolism (hyperparathyroidism, hyperphosphataemia, and hyper- or hypocalcaemia, etc.), protein energy malnutrition and anaemia. Fluid retention is a major clinical problem in patients with ESRD and has been directly linked to medical conditions such as hypertension, ventricular dysfunctions and other cardiovascular diseases, therefore having a significant effect in cardiovascular mortality [16]. Alterations to normal mineral metabolism begin to occur in the early stages of CKD and are fully present by the time patient develops ESRD, with hyperphosphataemia and hyperparathyroidism being regularly linked with mortality in dialysis patients [17]. ESRD patients are also at high risk of suffering from malnutrition, which can be characterized by an imbalance between nutrient requirement and intake resulting in the deficit of energy, more specifically, protein energy [18, 19]. The kidneys are the organ primarily responsible for the regulation of erythropoiesis, the process by which red blood cells are produced. Henceforth, a decrease in erythropoietin output by patients with renal failure, results in hypo-proliferative anaemia [20]. Iron deficiency due to frequent phlebotomy, inflammatory conditions due to infection, shortened lifespan of red blood cells and blood retention in the tubing of the dialyser during dialysis are some additional factors to be taken into account when it comes to the development of anaemia [2].

1.1 - Dialysis

Patient´s kidneys with ESRD only perform at 10 to 15 percent of their normal capability being unable to fulfil the tasks that they are supposed to do [13]. Since kidney transplants are not always an option and finding a suitable donor is a strenuous and long process, more than two thirds of people suffering from this disease resort to dialysis, which enables these patients to continue living for many years or even decades.

Hemodialysis (HD) and peritoneal dialysis (PD) (Figure 2.1) are the two main types of dialysis, and the most suitable for each person depends on individual medical factors, as well as, personal preferences. HD is typically done three times per week in dialysis centres (home HD is also an option) and involves the transportation of a patient’s blood out of the body to a

dialysis machine where it is filtered [21]. Contrarily, patients who undergo PD have their blood cleaned internally, in the abdominal cavity with the help of the dialysis fluid that it transported via an abdominal catheter [22]. This procedure is usually done at home and involves two different methods. In continuous ambulatory peritoneal dialysis, there is no need for external equipment since the dialysis fluid is manually exchanged a few times a day. On the other hand, there is also the possibility of doing automated peritoneal dialysis where the catheter is linked to a device responsible for exchanging the dialysis fluid. In both HD and PD, the patient is required to have an initial minor surgery for implanting a permanent catheter [22].

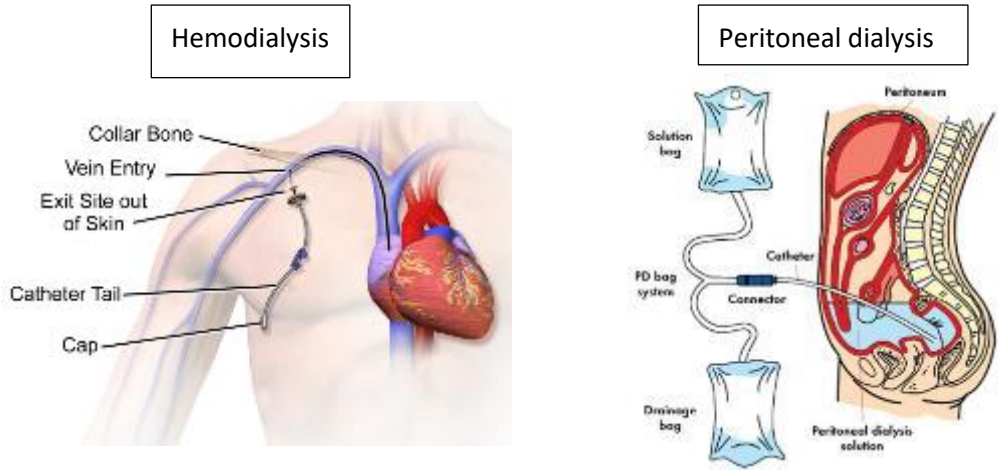

Figure 2.1 - Schematic representation that illustrates the differences between hemodialysis (HD) and peritoneal dialysis (PD). Adapted from [23].

1.1.1 - Catheter-related infections (CRIs)

Infections are the main cause of morbidity and the second cause of mortality, behind cardiovascular events in ESRD patients undergoing dialysis [8, 9]. Frequent disruption of the skin barrier during dialysis therapy that enhances exposure to potential risk factors, comorbid conditions (cardiovascular diseases, diabetes mellitus, etc.) and an acquired immune deficiency state of uremia, are some of the reasons that explain the high incidence of bacterial infections in patients with ESRD [24]. This incidence is so high that CRIs represent the third leading cause of hospital-acquired infections [25]. These type of infections occur after colonization of the catheter hub and/or lumen by microorganisms that are present in the patient's skin or external sources [25]. Septicemia accounts for more than 75% of reported infections with annual mortality values that can be 300 times higher in HD patients compared to the general population [26]. In PD, infection of the peritoneum (peritonitis), subcutaneous tunnel and catheter exit site are the most common cases, with peritonitis representing 61% of all catheter related problems [27, 28]. Gram-positive bacteria such as *Staphylococcus epidermidis* and *S. aureus* are the most common agents responsible for the development of PD-associated infections [28]. Although *S. epidermidis* is a skin commensal, it can also act as an opportunistic pathogen in immunosuppressed patients, being the most prevalent in CRIs [29]. Additionally, both species have biofilm-forming ability [30]. Biofilms are an aggregate of cells embedded within a self-produced matrix of extracellular substances that is able to adhere to surfaces, conferring bacteria resistance towards antibiotics and the immune response of the host. Current treatment protocol usually involves the removal and replacement of the catheter and the administration

of antibiotics as seen in Figure 2.2. However, this has been insufficient in most cases, mainly due to the emergence of antibiotic resistance [31, 32].

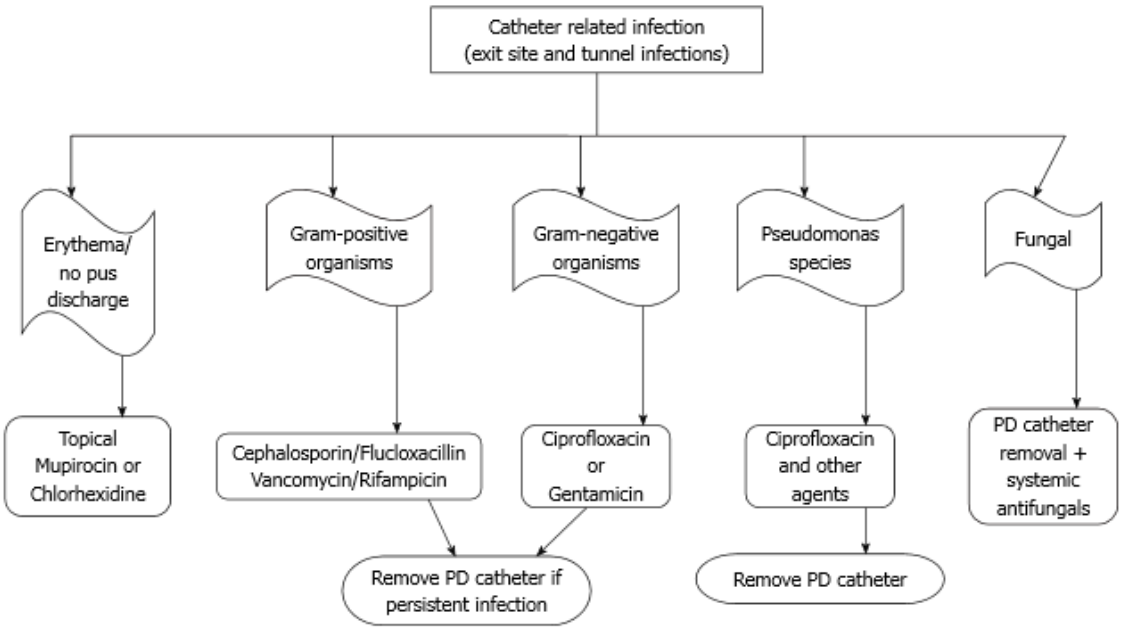

Figure 2.2 - Available treatments options for peritoneal dialysis (PD) catheter-related infections (CRIs). Adapted from [32].

1.2 - Antibiotic resistance Crisis

Alexander Fleming's discovery of penicillin back in 1928 set the dawn of the antibiotic age and the fight against infection-related diseases [33]. Some years later, bacterial resistance to penicillin started to become a clinical problem, which lead to the development of new beta-lactam antibiotics such as tetracycline in 1950, erythromycin in 1953 and methilicin in 1960 [34]. This time around it only took one year for the appearance of the first case of methilicin-resistant *Staphylococcus aureus*, in London in 1961 [33]. More recently, a novel antibiotic comprised of a combination of ceftazidime and avibactam was approved in 2015 for treating multidrug-resistant gram-negative infections. Nonetheless, in was reported in that same year the emergence of ceftazidime-avibactam-resistant *Klebiella pneumonia* [35].

This antibiotic resistance crisis has proven to have a direct link to the overuse of antibiotics due to inappropriate prescribing by physicians and their extensive use for agricultural purposes [34]. Unfortunately, what was considered one of the greatest advances in therapeutic medicine so many decades ago, has turned into one the most perilous threats of the 21st century with the increasing spread of antimicrobial resistance. Infectious diseases represent a major concern regarding public health, not only directly affecting the lives of millions of people but also putting serious strain on global economies [36]. According to a Centers for Disease Control and Prevention's report that came out this year, more than 2.8 million antibiotic-resistant infections occur every year in the Unites States alone [37]. Furthermore, antibiotic resistance is set to cause almost 300 million deaths by the middle of this century, which can also be translated into a loss of around 100 million dollars to global economies [37]. This situation is even more aggravated by the stall in the development of new

antibiotics by the pharmaceutical industry due to economic and regulatory obstructions (constant changes in regulatory and licensing rules, disparity in clinical trial requirements between countries and lack of clarity are some of the examples) [34]. Since antibiotics are developed with the intent of being curative and used for short periods of time, they are no longer considered to be profitable investments by pharmaceutical corporations [38].

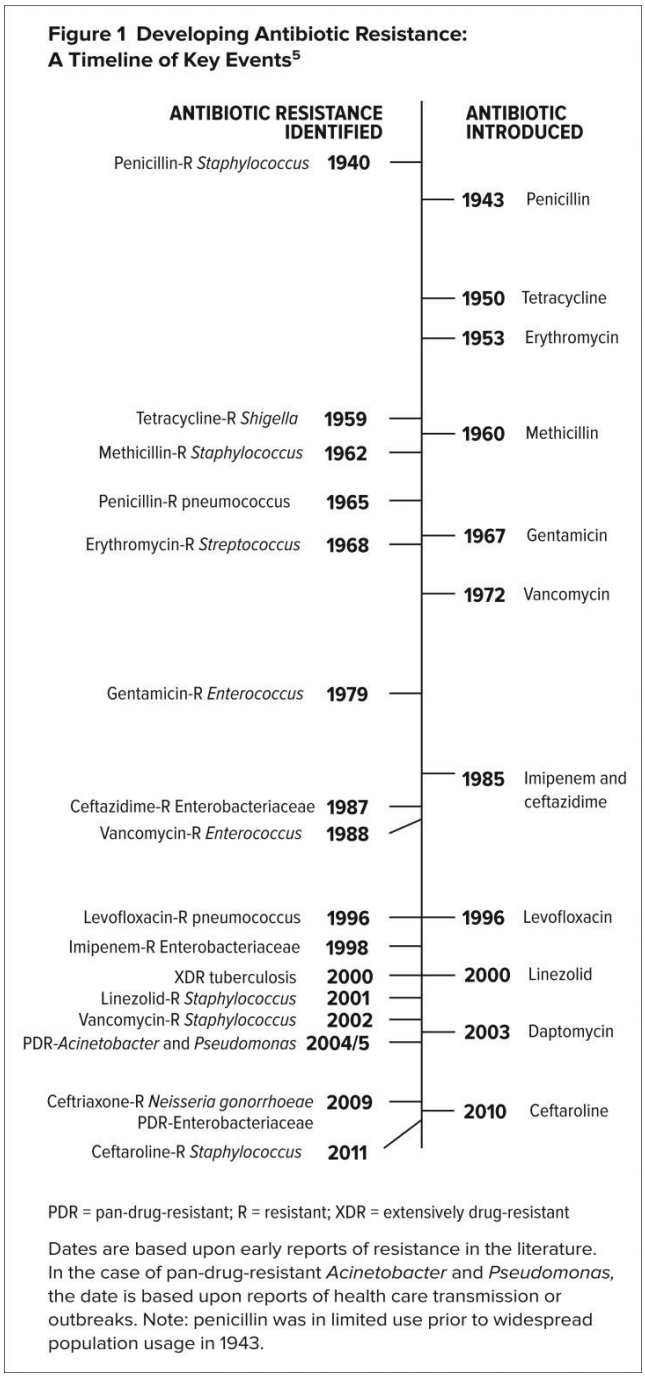

Figure 2.3 - Timeline concerning the development of antibiotics and concomitant appearance of antibiotic resistance. Adapted from [34].

In 2014, Gafor *et. al* conducted a 6-month study where he and his team identified the epidemiology of HD CRIs patients and tested different antibiotics against the specimens that were found. Results showed that 44.4% of the patients had gram-positive infections (main

organisms found were identified as *S. epidermidis* and *S. aureus*). Out of the 19 tested antibiotics only 2 of them, vancomycin and linezolid were completely effective against the gram-positive bacteria found [39]. This study is only a small proof of how big of a problem the emergence and development of antibiotic resistant bacteria is.

The rapid increase of this superbugs, their ever growing ability to resist current antibiotics, and spread resistance by gene mutations or exchange of genetic material between organisms [40], raise the demand for the discovery of new and non-traditional antimicrobial materials for a wide range of applications.

1.3 – Surface modification strategies to reduce catheter-related infections

Development of modified catheter surfaces to prevent and reduce CRIs has been raising a lot of attention as a possible alternative to the use of antibiotics. Since bacteria are able to adhere to the polymers (e.g., silicone and polyurethane) that are present in the surface of catheters, these can be modified in order to become anti-adhesive and/or bactericidal.

1.3.1 – Anti-adhesive coatings

Bacterial adhesion to surfaces can be affected by a variety of factors, including the inherent characteristics of the bacteria and the target material (e.g, surface charge and hydrophobicity), and the environmental factors of where the adhesion occurs (e.g, presence of proteins and pH) [41]. Conferring anti-adhesive properties to surfaces via modification of surface's chemistry and/or topography could result in reduced bacterial adhesion, which in turn could prevent the appearance of CRIs.

As most bacteria are negatively charged in neutral media, thus neutral and negatively charged surfaces are expected to reduce bacterial adhesion, in comparison with positively charged surfaces [42, 43]. Poly(ethylene glycol) (PEG) has a slightly negative to neutral net charge and also presents non-fouling behaviour [44]. Therefore, PEG and its derivatives have been extensively used for the development of anti-adhesive coatings (Figure 2.4) [44-47]. Nonetheless, current findings show that PEG chains interact with proteins in aqueous solutions via weak hydrophobic interactions, which facilitates bacterial adhesion and subsequent biofilm formation [48]. Zwitterionic polymers such as poly(sulfobetaine methacrylate) are also promising candidates for the preparation of anti-adhesive coatings as they have shown to inhibit bacterial adhesion by resisting protein adsorption [47, 49]. Likewise, polysaccharides like agarose and hyaluronic acid have been investigated as potential alternatives as they have demonstrated to inhibit bacterial adhesion [50, 51].

Anti-adhesive coatings do not kill bacteria and it is very difficult to guarantee that they are able to completely block bacteria from adhering to the surface of catheters. Even if only a few bacterial cells manage to adhere to the surface of the modified catheters, they can eventually form a biofilm, which will be followed by the development of infection. For that reason, anti-adhesive coatings that also offer bactericidal properties might be a possible solution.

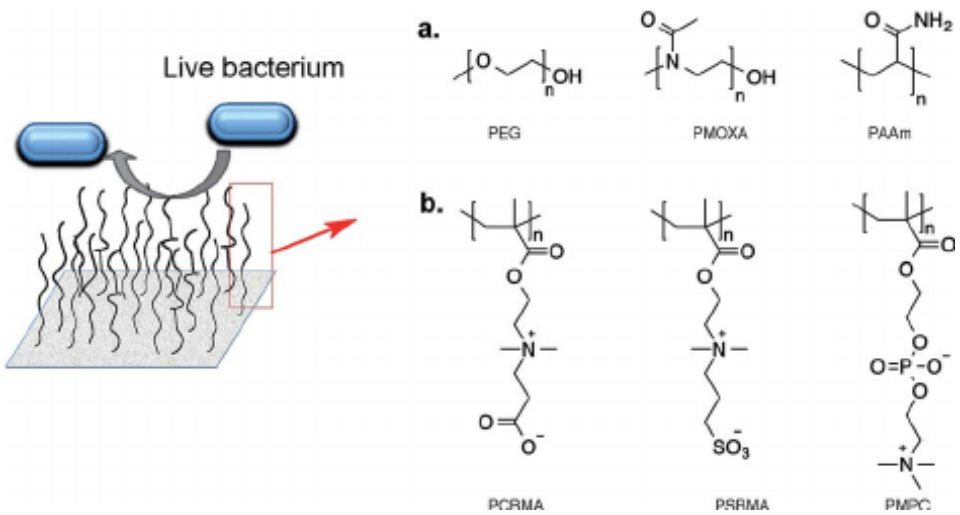

Figure 2.4 – Hydrophilic polymer brushes as anti-adhesive coating. Chemical structures of (a) neutral polymers and (b) zwitterionic polymers used for the development of anti-adhesive coatings. Adapted from [45].

1.3.2 – Bactericidal coatings

Bactericidal coatings can be developed using bactericide-releasing agents or by immobilizing antimicrobial agents on the surface of the coating [47]. Bactericide-releasing agents, also called eluting agents, are slowly released with the passage of time and are able to limit the growth and kill the bacteria that adheres to the surface as well as in the nearby surroundings (Figure 2.5) [47, 52].

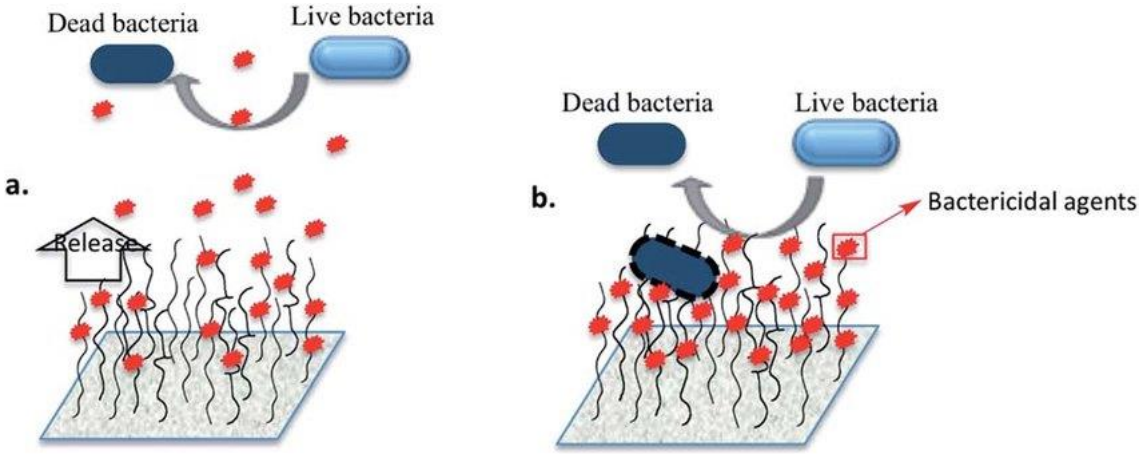

Figure 2.5 – Representation of (a) bactericide-releasing coatings and (b) contact killing coatings where bactericidal agents are covalently immobilized. Adapted from [45].

Silver nanoparticles [53, 54], nitric oxide (NO) [55] and antibiotics such as triclosan [56] and rifampicin [57] have been used as eluting agents in bactericidal coatings. These bactericidal agents can be incorporated into polyurethane (PU) used in dialysis catheters via casting methods [58, 59]. First, the PU material is dissolved with an appropriate solvent; subsequently the antimicrobial agent is added to the solution; finally, the solvent is evaporated. Another possible way to achieve this goal is to entrap the agents in preformed silicone objects [59]. By

dissolving the agents in solvents like chloroform, it is possible to impregnate the object with these solutions followed by solvent removal. Although these impregnation methods have shown some positive results, it also became clear that this strategy has some disadvantages when it comes to controlling the release rate of the agent and the amount of the agent that can be loaded onto the surface of the material [55]. This is particularly important as recent evidence shows that sub-inhibitory concentrations of bactericidal agents can be a determining factor in the devoplment of resistance by bacteria [60].

As stated before, another alternative is to covalently immobilize the antimicrobial agent to the surface of the material (Figure 2.5 (b)). This strategy offers the possibility of longer-term effects when compared to bactericide-releasing agents. Antimicrobial peptides (AMPs) [61, 62] and quaternary ammonium compounds (QACs) [63, 64] have been immobilized on surfaces as antibacterial coatings. However, investigations done with AMPs show that factors like lateral mobility, appropriate orientation and existence of spacer can greatly affect their antibacterial properties [65, 66]. QACs have been anchored to chitosan [64], hydroxylated surfaces [67] and poly(ethylene terephthalate (PET) films [68]. But because of their positive net charge, these compounds are likely to promote protein adsorption and subsequent bacteria adhesion, compromising their antibacterial efficiency [63]. The same problem applies to AMPs as they are also positively charged [69]. Therefore, the integrated utilization of anti-adhesive and bactericidal agents could be a solution to overcome these drawbacks. Lastly, graphene-based materials (GBMs) such as graphene oxide (GO) has also been incorporated with PU as antibacterial coatings. GO reinforced composite films made of polylactic acid (PLA) and PU, showed improved bacterial activity upon inclusion of the GO, with the incorporation of this material reducing bacteria growth up to 100% [70]. GO was incorporated with the PLA/PU films by liquid-phase mixing method, as it contains carboxyl groups that are able to covalently bind to the amine groups from the PU molecules. Furthermore, oxidized graphene nanoplatelets (GNPox) have also been incorporated with PU, as shown by a recent study by Borges *et al*. [71]. In here, GNPox-containing coatings were able to reduce bacterial adhesion by 70% while also achieving 70% of bacterial death. Unfortunately, several factors (e.g., size, orientation, exposure, edge density, wettability and level of oxidation) can greatly influence GBMs antibacterial activity [72].

2. Graphene-based Materials

2.1 - Structure and properties

Graphene-based materials (GBMs) are a somewhat recent class of nanomaterials [73]. They possess a remarkable set of characteristics that include superior mechanical strength, chemical stability, high surface area and thermal conductivity making them promising candidates for environmental and energy applications, but also in the field of biomedical aids, including biosensing, bioimaging and drug delivery [74-77]. Graphene (G), graphene oxide (GO) and reduced graphene oxide (rGO) are some of the main materials of this family, which also include graphene nanoplatelets. GBMs main materials are identified in Figure 2.6.

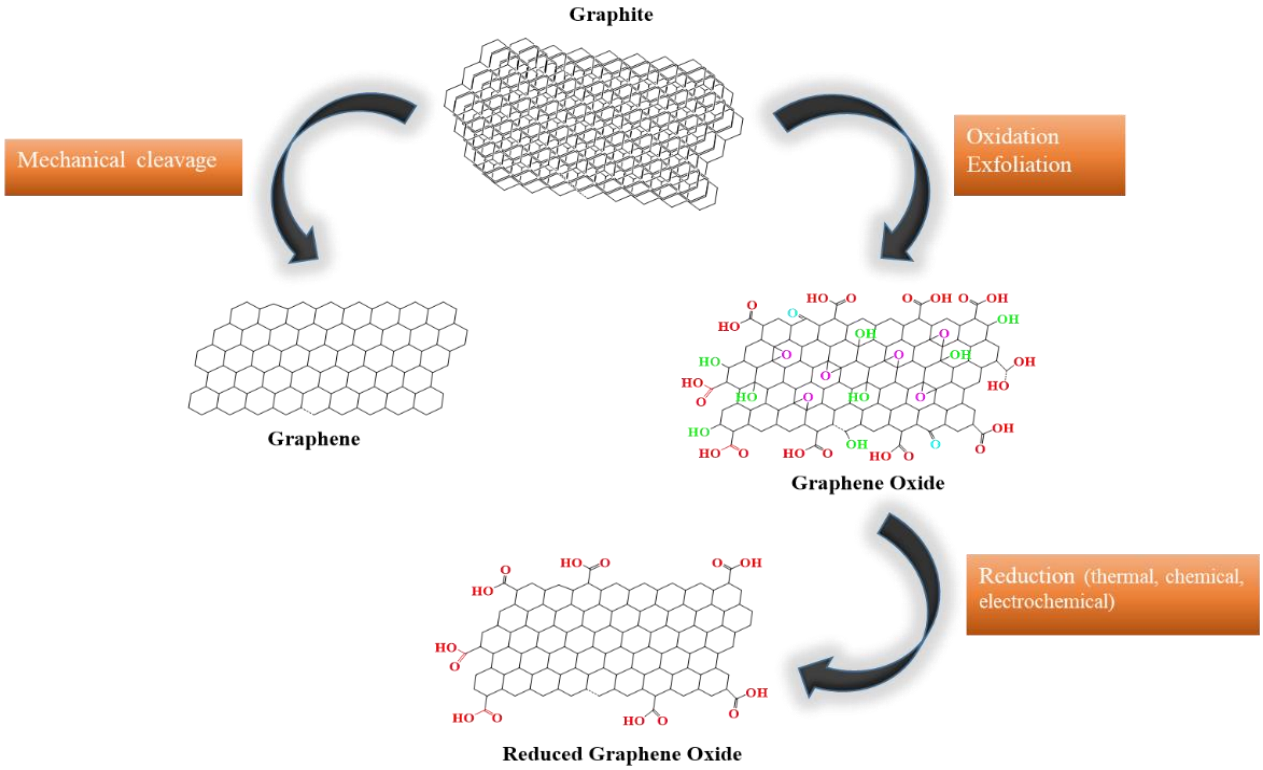

Figure 2.6 - Schematic representation of the main materials that comprise the family of Graphene-based materials (GBMs), as well as, some main synthesis processes that lead to their formation. Carboxyl groups (-COOH) appear in red, hydroxyls in green (-OH), epoxides (-COC) in purple and carbonyls (-CO) in blue.

G is an allotrope of carbon arranged in a 2D single planar sheet of tightly packed atoms in a sp^2 orbital hybridization, making it the thinnest material known to man [78]. Since its discovery in 2004 by Andre Geim and Konstantin Novoselov, research involving G has exponentially increased due to its physical (surface area up to 2630 cm^2/g), electrical (electron mobility up to 200.000 cm^2/g), thermal (up to 5000 W/mK of thermal conductivity) and optical (almost 98% of optical transmittance) properties resulting from long-range π conjugation [79].

G synthesis is done by two main approaches (Figure 2.7): top-down (destruction or successive cutting of precursors such as graphite) and bottom-up (assembly of other carbon sources to produce G) [80]. Some of the top-down methods include arc discharge, mechanical exfoliation and liquid-phase exfoliation, whereas the main bottom-up methods are chemical vapour deposition and epitaxial growth [79].

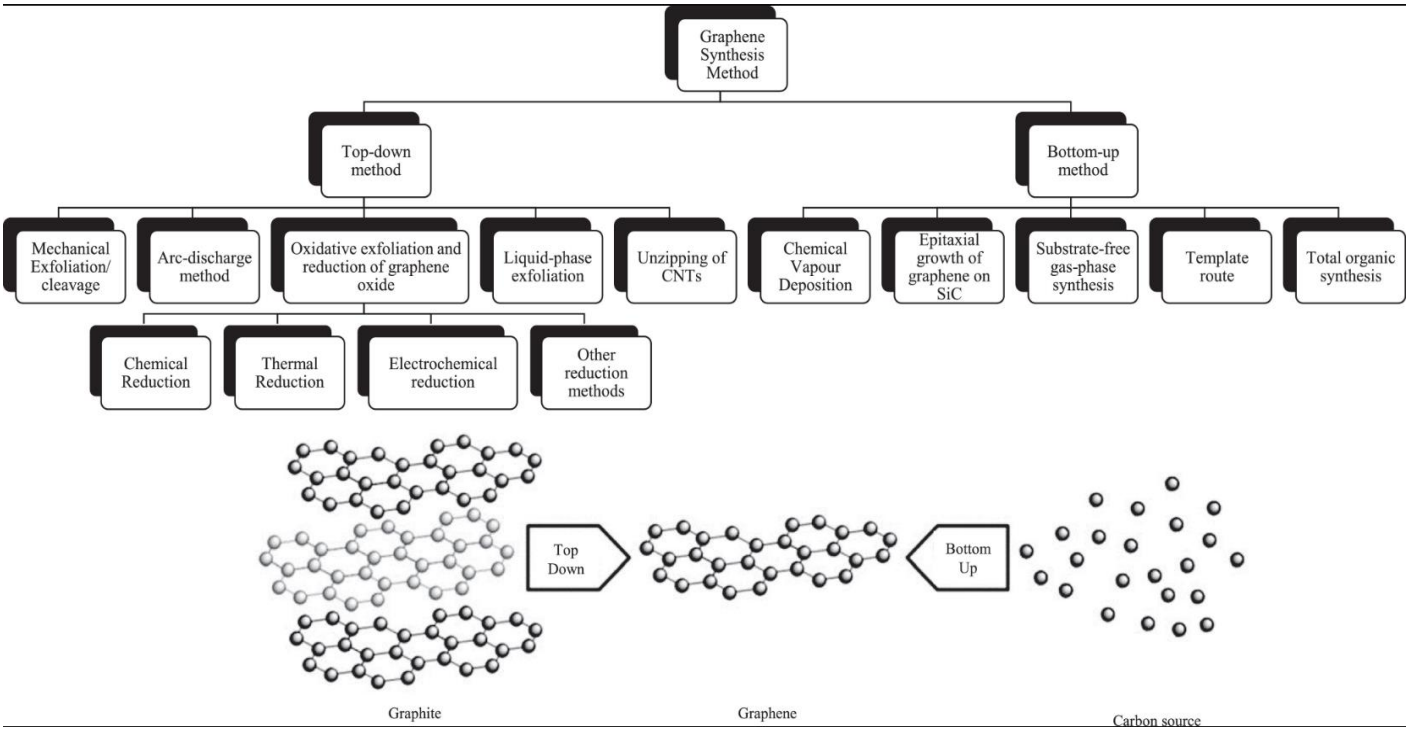

Figure 2.7 - Top-down and bottom-up methods for Graphene (G) synthesis. Adapted from [79].

In order to fine tune G to specific applications, it is usually modified [78]. Its oxidized form, GO, contains oxygen functional groups including carboxyl groups, epoxides, hydroxyls and carbonyls. The existence of these chemical moieties enables GO functionalization with biomolecules. This material is typically characterized by a C/O ratio that varies from 3:1 to 2:1 depending on the level of oxidation [81]. Inclusion of the oxygen functional groups causes partial destruction of the sp^2 structure and leads to sp^3 hybridization on some of the carbon atoms. This alteration in hybridization has practical effects on the original properties of G, as GO has lower electric conductance and does not absorb visible light, although it has higher chemical activity [82].

rGO is a cost-efficient and simple alternative to pristine G. Contrarily to pristine G production, which involves high cost procedures, being very difficult to scale at industrial levels, rGO can be easily obtained by reducing GO using high temperature treatments or reducing agents such as hydrazine hydrate and Zn powder [83, 84]. rGO is usually the material of choice for electrochemical sensors and similar applications as it is easier to produce at a larger scale by chemical reduction of GO [81]. rGO is structurally more similar to G than to GO, but it does contain some defects on the graphitic backbone, as well as, some residual oxygen atoms [81]. Due to the reduction process, this material presents a lower percentage of oxygen (higher C/O ratio) which leads to an increase of its hydrophobicity, making it more difficult to disperse in aqueous media in comparison to GO [83].

The differences regarding the dispersion of GO and rGO in aqueous solutions cannot be solely related to the presence of a superior concentration of oxygen functional groups. The underlying chemical nature of those functionalities also has a preponderate role on electrostatic stabilization by these materials' oxidized groups negative charges [85, 86]. In a study done by Konkena *et al*, zeta potential analysis showed that GO sheets achieve stable dispersions at pH values as low as 4 [86]. Contrarily, rGO sheets needed more basic conditions (above pH 8) to develop the necessary negative charge that allows for stable dispersion [86]. These findings can be explained by the ionization of different oxygen containing functional groups from both GO and rGO. In the case of GO, ionization of the carboxyl groups occurs at pH 4.3 and 6.6. The reason for two different pH values concerning carboxyl ionization are related to the hydroxyl groups in an ortho position that stabilizes the carboxylate anion. At pH 9.8 the ionization of the hydroxyl groups present in the graphitic backbone occurs. In the case of rGO, no phenolic hydroxyls and epoxide groups are usually present, since these are removed during the reduction process. Nevertheless, there are still some carboxylic groups that become ionized at pH 8 [86]. The ionization events for both GO and rGO are depicted in the figure below.

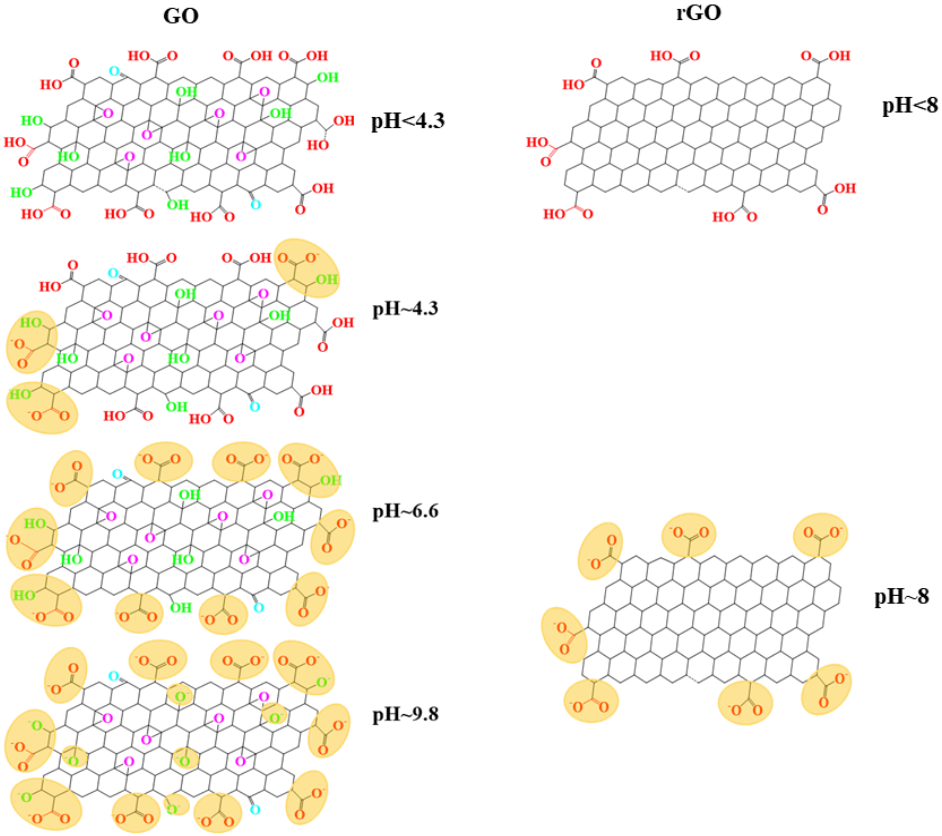

Figure 2.8 - Schematic representation of the ionization state of Graphene Oxide (GO) and reduced Graphene Oxide (rGO) at the indicated pH values. The ionized groups appear highlighted in the figure. Carboxyl groups (-COOH) appear in red, hydroxyls in green (-OH), epoxides (-COC) in purple and carbonyls (-CO) in blue.

2.2 - GBMs antimicrobial mechanisms

The antibacterial properties of G and its derivatives have been explored in recent years [81, 87, 88]. Although still not completely understood, G's antibacterial mechanisms have been suggested to have either a physical or chemical origin (Figure 2.9). Physical modes of action involve interaction of bacteria with the sharp edges of G. These can penetrate the lipid bilayer, decreasing the energy barrier required for disruption of bacterial membrane [89]. An additional physical mechanism denominated as wrapping has also been proposed. Due to the incredibly low thickness of G (world's thinnest material), it can act as flexible barrier isolating bacteria from their surroundings, limiting their nutrient supply, which could lead to bacterial growth inhibition and concomitant death [90]. On the other hand, G can induce oxidative stress by its basal planes, liberating reactive oxygen species (ROS) such as hydroxyl radicals, superoxide radicals and hydrogen peroxide, which chemically deactivates bacterial proteins and lipids, therefore inhibiting bacteria proliferation [89, 90]. Furthermore, G is also able to compromise the integrity of the bacterial membrane by removing electrons from it, since it can act as an electron acceptor [91]. Both GO and rGO maintain the characteristic antimicrobial properties of G [87, 92, 93].

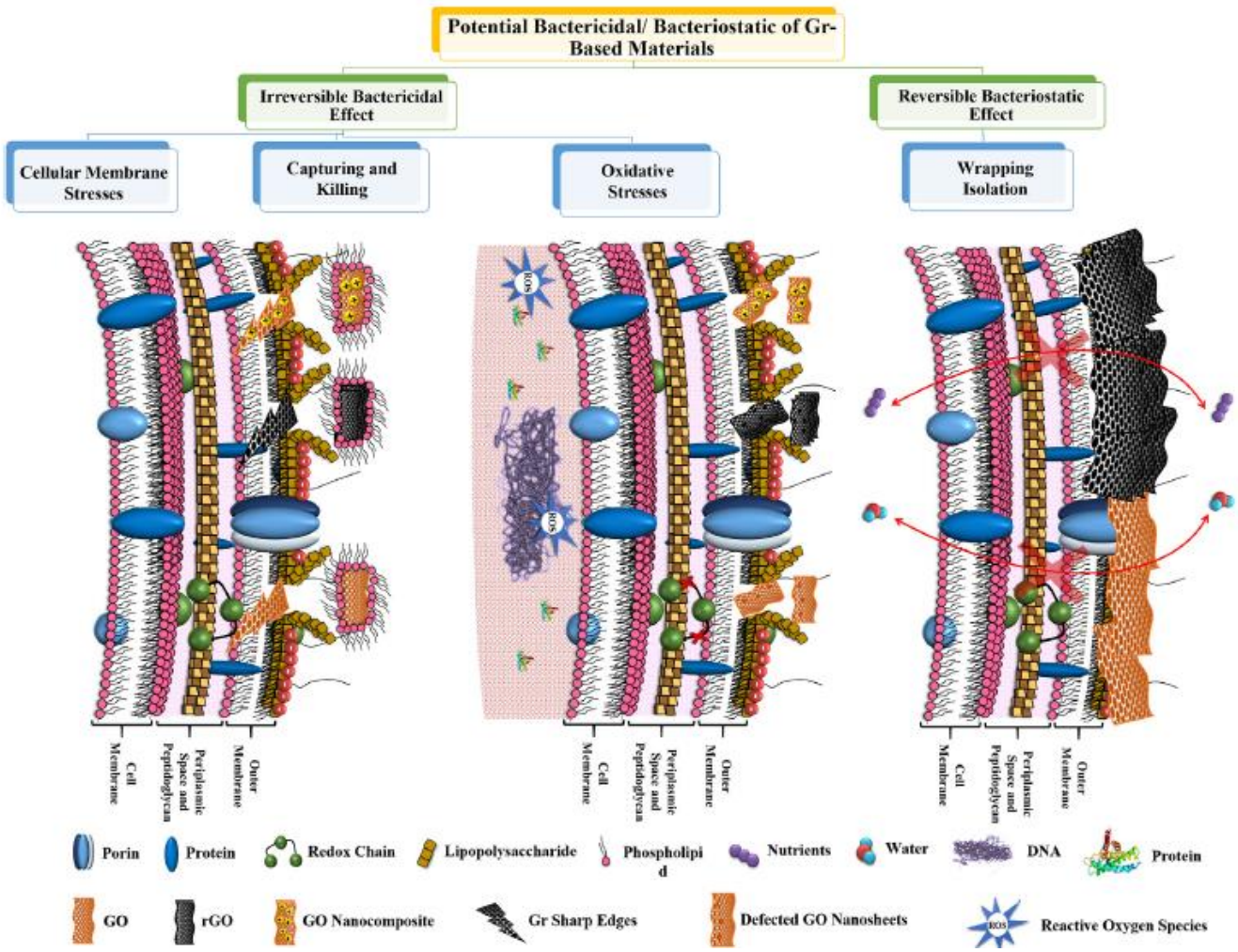

Figure 2.9 – Graphene-based materials (GBMs) mechanisms of action. Adapted from [94].

3. Antimicrobial Peptides

3.1 – Origins and main characteristics

Antimicrobial peptides (AMPs) are a heterogeneous family of peptides, first discovered in the 1980's and that can be found virtually in all organisms [95]. AMPs have been at the forefront of host defence for millions of years [96]. They are important components of the host's innate immunity system and are critical in fighting off infections [96, 97]. AMPs key features include small size (up to 50 amino acids) with molecular weights (MW) that usually do not surpass 5kDa, cationic character (net charge of +2 to +9) and an amphipathic behaviour [98]. A great advantage of many AMPs is the fact that they present exceptionally broad range of antimicrobial activity, not only covering gram-positive and gram-negative bacteria but also other microorganisms, such as viruses and fungi [99]. Furthermore, since most AMPs target the bacterial membrane, it is less probable for bacteria to develop resistance, as they would have to redesign the composition of the lipids present in the bacteria membrane, an energy exhausting process [69].

However, AMPs' lack of stability under physiological salt concentrations, high susceptibility to proteolysis, and toxicity towards eukaryotic cells at high concentrations hinders their use when systemic administration of the peptide is needed, favouring therefore their local application instead [95, 100]. A strategy to overcome these limitation could be the AMPs immobilization onto a material for local application, providing antimicrobial properties while promoting AMPs stability and biocompatibility [69].

3.2 - Structure of AMPs

AMPs can be categorized based on their secondary structures, being the most common α-helix and ß-sheet (Figure 2.10) [101]. α-helix structure is characterized by the presence of two adjacent amino acids distanced by 0.15 nm with an 100 degree angle between them [102]. The activities of this class of AMPs can be related to the large variety of helical structures as these depend on length of the helix, content and orientation of the residues by which they are formed [103]. Magainin, protegrin and indolicidin are some of the best examples of AMPs that belong to this category [102]. On the other hand, ß-sheet AMPs have disulphide bonds that link the existing ß-sheets [104]. These AMPs can be further subcategorized into ß-hairpin peptides and α-defensin peptides based on their cysteine content [103]. Additionally, there are AMPs that do not belong to none of the above-mentioned classes, as some have structures that contain a combination of both α-helix and ß-sheet elements and others that assume an extended conformation.

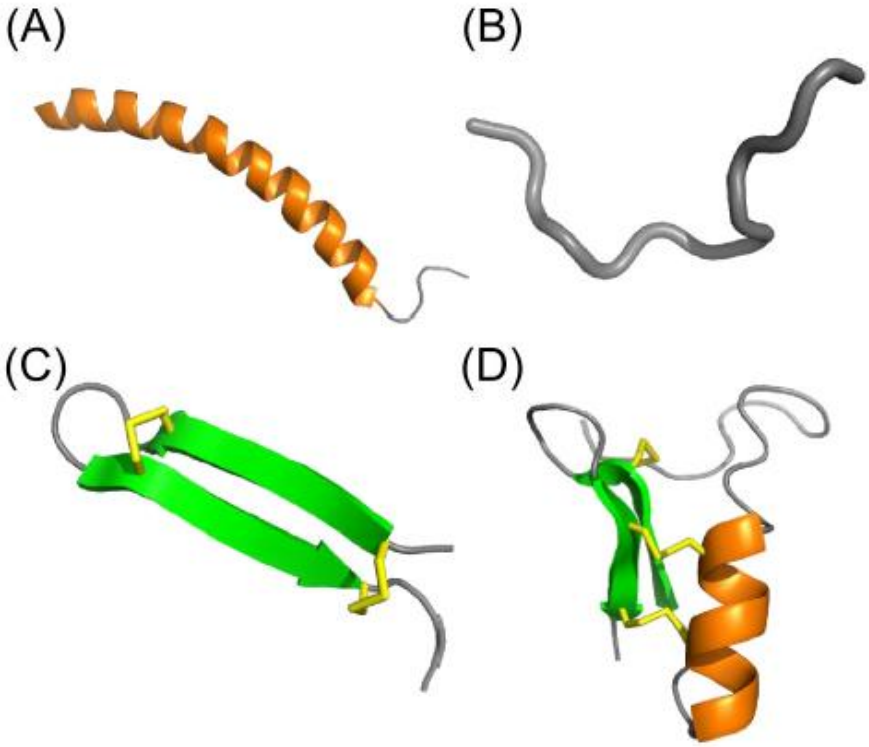

Figure 2.10 - Common Antimicrobial peptides (AMPs) structures: (A) α-helix; (B) extended; (C) ß-sheet; (D) AMPs with α-helical and ß-sheet elements. Adapted from [103].

3.3 - AMPs antimicrobial mechanisms

Although there is still debate regarding AMPs mechanism of action towards bacteria, it is accepted that positively charged AMPs are able to electrostatically bind to the negatively charged phospholipids of the outer leaflet of the bacteria's cytoplasmatic membrane, despite the significant differences between Gram-positive and Gram-negative cell envelope structure [105, 106]. Gram-negative bacteria possess an additional outer layer that surrounds its cytoplasmatic membrane. Therefore, AMPs first undergo a process designated as self-promoted uptake where the peptide displaces divalent cations Ca^{2+} and Mg^{2+} and bind to the lipopolysaccharides present in the outer membrane due to the increased affinity for this molecule [107]. This displacement leads to permeabilization of the membrane which in turn allows for the passage of the AMP that is now able to reach the cytoplasmatic membrane [95]. How this interaction leads to bacterial death is yet to be fully determined, but leakage of cellular contents due to the creation of physical holes, extreme depolarization of the bacterial membrane, promotion of the degradation of the cell wall by hydrolases and damage to intracellular targets after internalization of the AMP have been presented as possible explanations [95]. It is possible that more than one of these mechanisms to occur simultaneously, producing a synergistic effect [98, 108, 109].

Current models that account for the mechanism of action of membrane-active AMPs can be seen in Figure 2.11 and include: (a) barrel-stave pore model; (b) toroidal pore model, (c) carpet model and (d) detergent model [110]. Both barrel-stave and toroidal models encompass the formation of transmembrane pores on the cytoplasmic membrane, but whereas the former requires peptide-peptide interactions for the formation of the pore, the same is not observed in the latter as the peptides and phospholipids' head groups induct a curvature of the lipid bilayer resulting in pore formation [69, 101]. Another main difference between these two models is related to the arrangement of the lipid bilayer, since the barrel-stave structure allows for the maintenance of the hydrophilic and hydrophobic arrangement and the toroidal structure does not. The carpet model involves the reduction of the membrane thickness due to a saturation of adsorbed peptides that ultimately causes the lysis of the cellular membrane [69, 101]. The detergent model represents a similar mechanism to the last one, but involves high concentrations of AMPs having a detergent-like effect that causes formation of micelles comprised of peptides and lipids resulting in the degradation of membrane integrity [35, 69, 111].

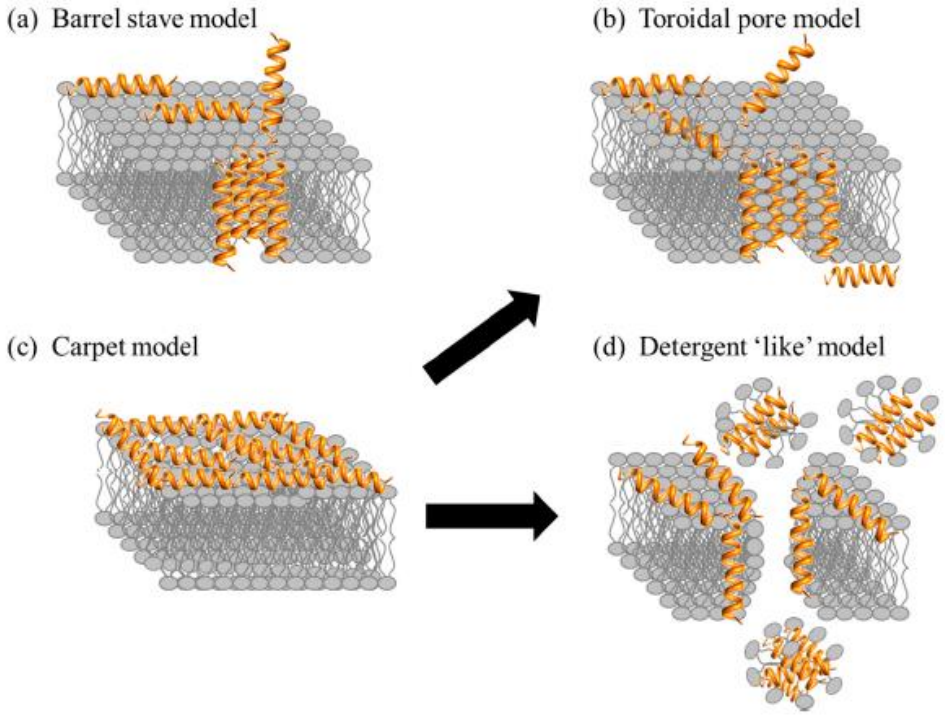

Figure 2.11 - Current proposed models for mechanisms of action of membrane-active Antimicrobial peptides (AMPs): (a) Barrel stave model, (b) Toroidal pore model, (c) Carpet model, (d) Detergent "like" model. Adapted from [110].

4. Conjugating GBMs with AMPs

4.1- Non-covalent interactions between GBMs and AMPs

Combining GBMs with AMPs offers the possibility of leveraging the important characteristics of these materials, with enhanced antimicrobial activity, important to a vast range of biomedical applications.

When adsorbing a peptide to graphene, one should consider the structural and chemical diversity of the interface created by peptide presence. A peptide's binding mode through non-covalent adsorption can be difficult to predict since it depends on a combination of molecule-substrate, molecule-molecule and molecule-solvent interactions [112]. Nonetheless, non-covalent or supramolecular functionalization of G and its derived materials is sometimes preferred over covalent functionalization since it does not have any effect over graphene's structural, electronic and optical properties while also allowing for the incorporation of new elements [113]. Non-covalent modification englobes several forces including π-π interactions, van der Waals forces, electrostatic force and hydrogen bonding [114]. Relative strength of non-covalent interactions could be seen as disadvantage in comparison to covalent approaches since the dissociation energies of individual supramolecular interactions are usually lower than of covalent bonds, making it easier for a molecule (in this case, a peptide) to dissociate from G [114]. Nevertheless, if the number of non-covalent interactions is large enough (G's incredibly large surface may offer this possibility), the overall non-covalent binding energy can rival some covalent bonds [114]. Moreover, this relative lack of strength from non-covalent interaction can also prove to be useful in cases where the release of peptide over time from the graphitic material is desirable, so it largely depends on the specific aim of the hybrid material in question.

To the best of our knowledge only Mannoor and co-workers reported functionalization of a GBM with an AMP via non-covalent interactions [115]. The aim of the work was to design a wireless AMP conjugated G biosensor that could be printed onto bioresorbable silk and, in turn, detect specific bacterial species on tooth enamel. This biosensor is depicted in Figure 2.12. Here, a bifunctional peptide consisting of a dodecapeptide graphene-binding peptide (GBP), a triglycine linker and the AMP odoranin-HP (HSSYWYAFNNKT-GGG-GLLASSVWGRKYYVDLAGCAKA) was non-covalently self-assembled onto G, to form a G-AMP composite. The GBP moiety of this bifunctional peptide is responsible for the adsorption process showing strong non-covalent interactions with G's surface, whereas the AMP at the tail end contributes for the binding of the pathogenic bacteria. In fact, the choice of this GBP was not random since it had previously shown to be able to uniformly cover the surface of graphene due to π-π interactions in the work done by Kim and his team [116]. The adsorption process was confirmed by labelling the bifunctional peptide with fluorescein isothiocynate and by conducting Raman spectroscopic analysis of the modified G, which indicated doping of the material. The biosensor tested positive for the detection of *S. aureus* in an intravenous bag with a detection limit of 1

bacterium per microliter of blood, and *H. pylori* in human saliva with a lower detection limit of around 100 cells.

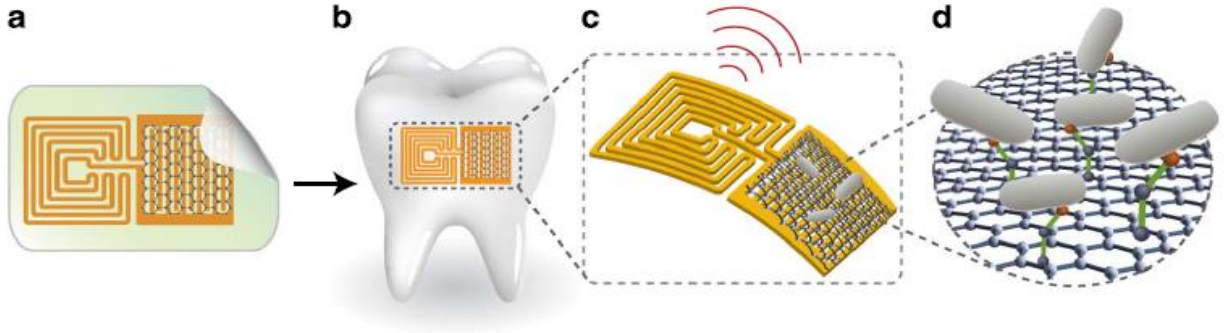

Figure 2.12 – Wireless Antimicrobial peptide (AMP) conjugated Graphene biosensor.(a) Graphene and wireless coil are printed onto bioresorbable silk. (b) Placement of the biosensing platform onto the surface of the tooth. (c) Detailed schematics of the biosensing platform. (d) Binding of bacteria by the bifunctional peptide self-assembled on top of the graphitic backbone. Adapted from [115].

4.2 - Covalent Interactions between GBMs and AMPs

A review of current literature on ways to covalently bind AMPs with GBMs showed that most groups resort to strategies that couple carboxyl groups (-COOH) of GO and the primary amines (-NH_2) of AMPs via 1-ethyl-3-(3-dimethylaminopropyl)carbodiimide/*N*-hydroxysuccinimide (EDC/NHS) coupling chemistry, in a reaction commonly known as amidation. Although less used, we have found cases where copper(I)-catalyzed azide-alkyne cycloaddition (CuAAC) "click" chemistry and even Michael addition reaction were used to successfully conjugate GBMs with AMPs. These chemical reactions will be explained and the most relevant papers that used one of these different approaches will be presented (table 2.2).

Table 2.2- Overview of Antimicrobial peptides (AMPs) immobilization strategies onto Graphene-based materials (GBMs), their applications and antimicrobial activities.

AMP immobilization strategy	GBM	AMP	Application	Microorganisms assessed	Antimicrobial activity	
EDC/NHS	GO	Nisin (NIS)	Antibacterial material for water treatment	*Staphylococcus aureus*	Colony plating technique: - Pristine GO had negligible antibacterial activity; - GO/NIS killed almost 100% of bacteria.	[117]
EDC/NHS	GO	ε-poly-L-lysine (PLL)	Antibacterial material for water treatment	*S. aureus; Klebsiella pneumoniae*	LIVE/DEAD assay: - PPL killed 55% of all bacteria at 100 μM; - GO/PLL killed 100% of all bacteria at 100 μM. Note: minimal inhibitory concentration (MIC) for ε-PL was determined to be 220 μM against *Staphylococcus aureus* and 175 μM against *Klebsiella pneumonia.*	[118]
EDC/NHS;	GO	PLL; NIS	Antibacterial material for water treatment	*Bacillus subtilis* 6633; *Escherichia coli* K12	Bacterial growth curves: - GO, GO/NIS and GO/PLL did not completely inhibit *B. subtilis* and *E. coli* growth; - Increased lag phase when testing GO/NIS (9h, as opposed to 1h from GO)	[119]
EDC/NHS	GO	Indolicidin (IN)	Antifungal therapy	*Candida albicans* ATCC 10231	Broth microdilution assay: - IN exhibited a MIC value 12.5 μg/mL; - GO exhibited a MIC value of 6.25 μg/mL; - GO/IN exhibited a MIC value of 3.12 μg/mL.	[120]
EDC/NHS	hrGO	Magainin I	Bacterial sensor	*E. coli* O157:H7	-	[121]
CUAAC	GO	HH36	Antibacterial biomedical material	*E. coli* ATCC 15224; *S. aureus* ATCC 29213	Colony plating technique: - Pristine GO had negligible antibacterial activity; - GO/HH36 killed 80% of all bacteria at a concentration of 80 μg/mL.	[122]
Michael addition reaction	rGO	NRC-03	Photothermal therapy	-	-	[123]

4.2.1 - EDC/NHS coupling chemistry

Carboxyl groups and amines work together as nucleophilic partners. Unfortunately, carboxyl groups are not very reactive, so activating them is an extremely important step to enhance their reactivity towards nucleophiles [124]. The most common strategy to achieve this goal involves using carbodiimide reagents, such as 1-ethyl-3-(3-dimethylaminopropyl)carbodiimide (EDC) [125]. The first step in activating a carboxyl group with a carbodiimide reagent implicates the formation of an *O*-acylisourea intermediate, which is a much more electrophilic compound and is now able to readily react with strong nucleophiles such as primary amines [124]. Nevertheless, an undesired effect in the formation of this intermediate compound is the fact that it is also reactive towards water molecules, which may cause the *O*-acylisourea to react preferably with the water molecules instead of with the intended nucleophile. Enhancing *O*-acylisourea's stability in order to promote the creation of amide- linkages is done by using an additional coupling reagent as *N*-hydroxysuccinimide (NHS) [125]. This leads to the formation of an ester that is more stable than the intermediate compound. Therefore, using NHS increases the reaction rate of the now activated carboxyl groups with the target nucleophile. This mechanism is excellently explained by Kasprzak *et al*. [124] and can be seen in Figure 2.13.

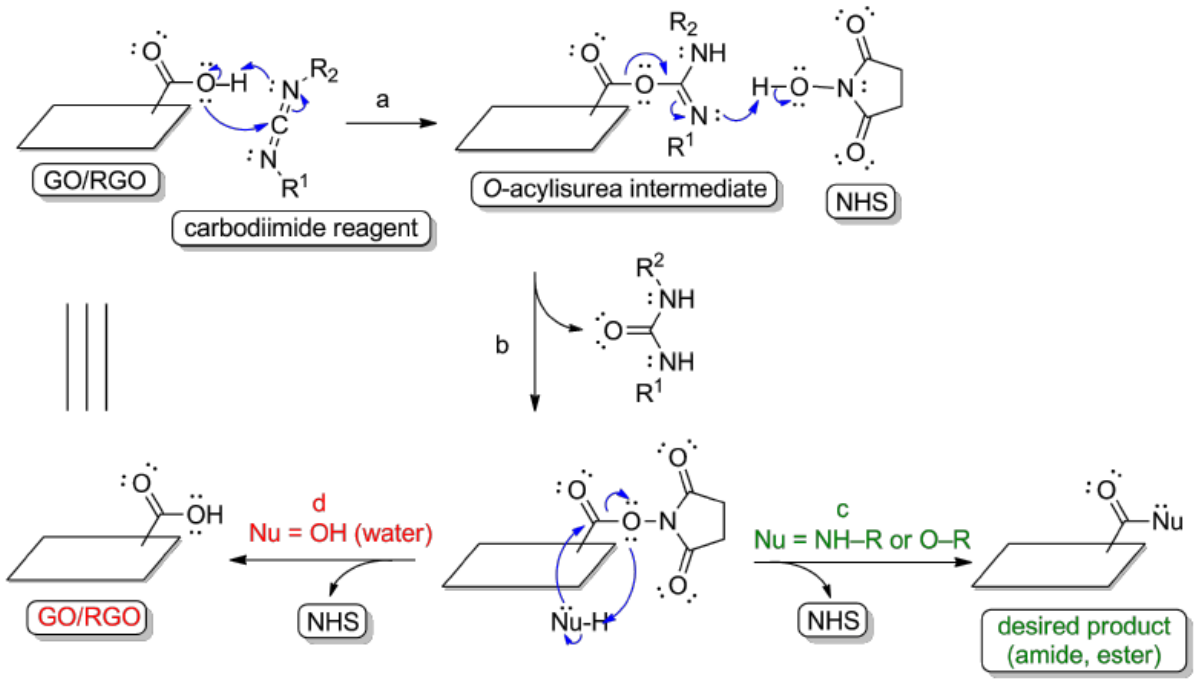

Figure 2.13 - Representation of graphene-based materials' carboxyl groups activation mechanism by EDC and NHS. (a) carboxyl group activation by a carbodiimide reagent, (b) stabilization of the *O*-acylisourea intermediate with NHS, (c) esterification/amidation reaction with desired nucleophile, (d) nucleophilic attack of the activated carboxyl groups by water molecules. Adapted from [124].

Through a bottom-up strategy, Kanchanapally *et al* developed 3D GO foam-based membrane conjugated with nisin, a polycyclic AMP most commonly used as a food preservative, with the intention of removing and killing multiple drug-resistant bacteria [117]. For this purpose, nisin (NIS) was firstly coupled with the 2D GO (single platelet) using the cross-linking chemistry EDC and NHS. After attaching NIS to the 2D GO membrane, amine functionalized PEG was used as a linker in order to develop a solid and porous 3D nisin-conjugated GO membrane,

using the same chemistry, as depicted in Figure 2.14. The material's antimicrobial efficiency was tested by washing the membrane's surface with 100 mL of contaminated drinking water with 8.9 x 10^6 colony-forming units (CFU) mL^{-1} of methicillin-resistant *Staphylococcus aureus* (MRSA) and the number of live bacteria was estimated by colony plating. The same test was done for a membrane without nisin. Results indicated that almost 100% of MRSA was killed using the AMP attached GO membrane, whereas the unmodified GO membrane showed that 92% of the MRSA was still alive.

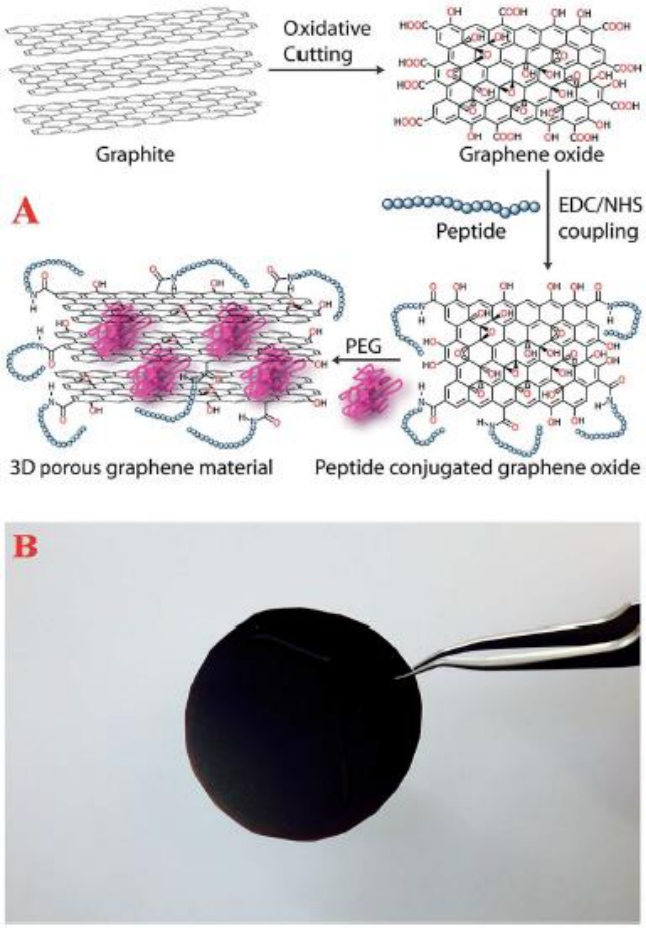

Figure 2.14 - (A) Schematic representation of the formation of nisin functionalized 3D Graphene Oxide (GO). (B) Photograph of the nisin functionalized 3D GO foam membrane. Adapted from [117].

More recently, Pramanik *et al.* followed a similar bottom-up approach for the development of 3D composites comprised of polydopamine nanoparticles (PDNPs), GO, and epsilon-poly-L-lysine (PLL), a natural cationic AMP known for killing microorganisms via cell membrane disruption [118]. After developing the PDNPs, these were attached to GO via EDC/NHS chemistry. This step was followed by adding PLL to the modified GO also via EDC/NHS coupling chemistry to form the 3D composite nanoparticle. The composite's ability to kill superbugs such as ß-lactamase producing *Klebsiella pneumonia* and MRSA were tested by colony plating technique and live/dead assay. The same experiment was performed with the PDNP-GO composite nanoparticle free of AMP. Results showed that AMP immobilization on the composite led to the death of 100% of the *K. pneumonia* and MRSA, when using 100 µM of the AMP for composite formation, whereas at that same concentration the AMP by itself could only kill 55% of all bacteria and the composite without the AMP was only able to kill less than 20%. It should

also be noted that the minimal inhibitory concentration (MIC) for PLL was determined to be 175 μM for *K. pneumonia* and 220 μM for MRSA.

Both Kanchanapally's and Pramanik's groups used Fourier transform infrared spectroscopy (FTIR) to access the immobilization efficiency of their respective AMPs onto GO. FTIR spectra of both groups display the appearance of peptide Amide A band at ~3350 cm^{-1} and Amide II at approximately ~1550 cm^{-1}, which can be attributed to N-H stretching vibration and in-plane N-H bending vibration from the peptide, respectively. More importantly though, is the appearance in Kanchanapally's spectrum of a strong peak at ~2300 cm^{-1} corresponding to –NCO vibration that can be correlated to the formation of amides between the peptide $-NH_2$ groups and the GO $-CO_2H$ groups, therefore confirming AMP immobilization. The same peak was not observable in Pramanik's spectra, which might indicate that the peptide is present but it does not confirm how it is linked to the GO surface.

A possible explanation for the antimicrobial test results from these first two works could be a synergistic effect between GO and AMP, by which GO is able to hold down bacteria by a mechanical wrapping process, causing stress and physically damaging cell membranes, and further enabling electrostatic binding between the AMP and the bacteria's negatively charged membrane.

Filina and co-workers combined both PLL, nisin and the antimicrobial enzyme lysozyme to covalently functionalize the surface of GO nanosheets with the aim of developing a novel material for water treatment [119]. Since all three antimicrobial agents have amino groups, EDC/NHS coupling chemistry was used to allow immobilization onto the nanosheets. Curiously, the group also attempted non-covalent functionalization of the GO nanosheets by electrostatic interactions, but it was found to be less effective (data was not presented in article). GO nanosheets functionalization was confirmed by Zeta potential and X-ray photoelectron spectroscopy (XPS). With the first technique a significant increase of the zeta potential was observed after antimicrobial agents introduction, suggesting its successful immobilization. Regarding XPS measurements, the presence of nitrogen further confirmed the presence of the antimicrobial agents on the composed samples. Moreover, the atomic percentage of nitrogen would double when doubling the amount of NIS and PLL used during the functionalization reaction, which confirms that the antimicrobial agents were present, but does not clarify if they were covalently linked to the GO via EDC/NHS coupling chemistry. The antibacterial activity of the pristine and functionalized GO nanosheets was evaluated from bacterial growth curves using Gram-positive *Bacillus subtilis* and Gram-negative *Escherichia coli*. Complete inhibition of growth was not achieved by none of the tested materials when using the *B. subtilis*, although there were changes to the growth behaviour of the bacteria such as increased lag phase (almost 9 hours for the NIS functionalized GO when compared to less than 1 hour for pristine GO) and slower growth rates. The same results were verified when using the *E. coli* model, although only the pristine and PLL functionalized GO were tested.

An additional example of immobilization of an AMP onto GO's surface via EDC/NHS coupling chemistry, can be found in the work produced by Farzanegan's group in 2018 [120]. In this case, Indolicidin (IN), one of the smallest natural linear AMPs and a member of cathelicidin family, was conjugated with GO to test its antifungal activity against *Candida albicans*, an opportunistic pathogenic yeast that causes candidiasis in immunocompromised individuals. The antimicrobial tests performed showed that IN and GO present MIC values 12.5 μg/mL and 6.25 μg/mL, respectively, when tested by themselves. Remarkably, the nanocomposite presented a much higher inhibitory effect with a MIC value of only 3.12 μg/mL. These findings suggest that

the conjugation of GO with IN might evoke a synergistic effect, leading to a higher efficiency against fungi.

Lastly, Chen *et al.* developed a field-effect transistor (FET) biosensor capable of detecting gram-negative bacteria [121]. The biosensing platform, comprised of reduced graphene oxide (rGO) covalently functionalized with the AMP Magainin I (GIGKFLHSAGKFGKAFVGEIMKS) via EDC/NHS coupling chemistry. FET sensors functioning involves changing the charge distribution of the semiconductor material when charged-molecules bind to the bio-sensitive layer [126]. In this case, rGO was used as the semiconductor component and Magainin I as the bio-sensitive layer. When the positively charged Magainin I binds to anionic lipopolysaccharides on Gram-negative bacteria's membrane, the charge distribution at the surface is changed, causing a corresponding shift in the electrostatic potential of the semiconductor (rGO). This shift in the surface potential leads to an alteration in the conductance between the source and the electrodes, which can then be measured. The device displayed a limit of detection of 803 CFU/mL when exposed to *E. coli*. The AMP-functionalized device was also exposed to Gram-positive *Listeria* cells as a control experiment. There was negligible change in the transfer characteristics, which indicated that there was minimal binding between Magainin I and the bacterial cells, further indicating the selectivity of the biosensor.

These reports show that EDC/NHS coupling chemistry is indeed an simple and efficient strategy to functionalize GBMs with AMPs, as it does not require any type of modifications to the starting materials and allows the formation of a stable covalent bond (amide bond) between the peptide and the graphitic material.

4.2.2 - Copper(I)-catalysed azide-alkyne cycloaddition (CuAAC) "click" reaction

CuAAC is a type of "click" reactions and involves the functionalization of substrates with other compounds via a triazole ring formation [127]. For CuAAC reaction to occur, three initial components are required: a terminal alkyne, an azide and a Cu(I) catalyst. The reaction begins with the formation of a Cu(I) acetylide with the nucleophilic alkylated nitrogen reacting with the backbonding metal (Figure 2.15). The triple bond from the terminal alkyne is a π donor, therefore it can react with the electrophilic centre from the terminal nitrogen of the azide, forming a metallacycle complex after the formation of the C-N bond. This leads to the oxidation of the Cu centre from oxidation state +1 to +3. Cu(III) is reduced back to Cu(I) due to ring contraction and a cuprous triazolide compound is obtained. To complete the formation of the triazolide the complex acquires a proton while releasing the Cu centre for the next catalytic cycle [128, 129]. CuAAC might represent a viable approach for immobilizing AMPs onto GO if the necessary modifications are made to the peptide and the graphitic backbone. "Click" chemistry is a class of high-yield and specific reactions that allows for the bioconjugation of

two biocompatible molecular building blocks via covalent binding. These are typically done in a single pot and generate little to no by-products [130].

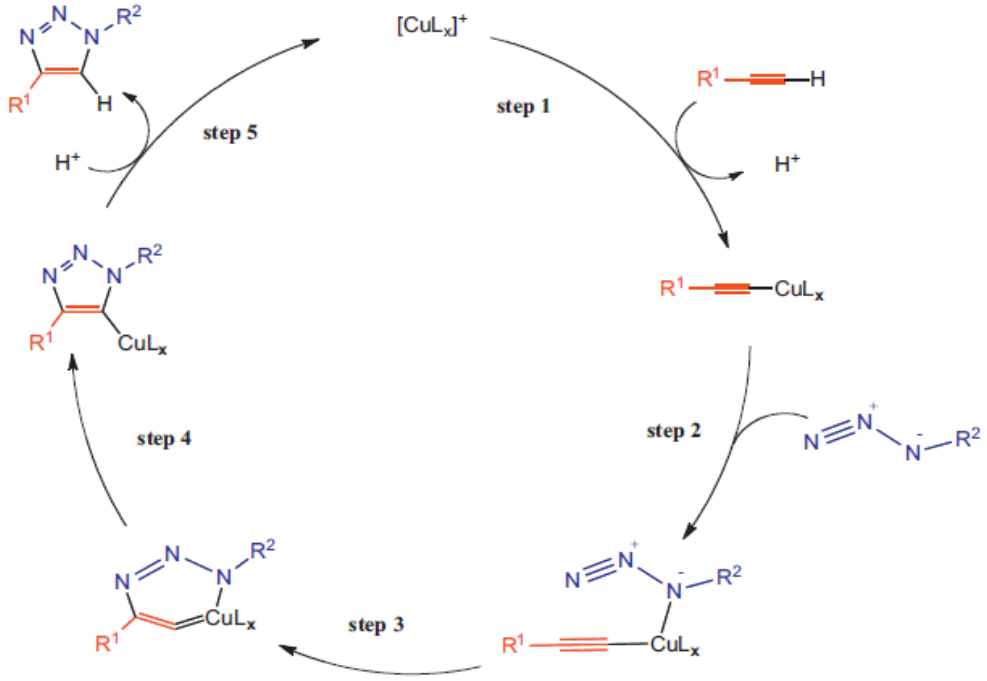

Figure 2.15 – Copper(I)-catalyzed azide-alkyne cycloaddition (CuAAC) reaction cycle mechanism proposed by Fokin and Finn's. Adapted from [131].

Shi *et al*. successfully immobilized an AMP (HHC36) onto GO via CuAAC "click" reaction [122]. Since GO does not naturally possess alkyne groups, the first step involved converting a big percentage of the existing hydroxyl groups into alkynes via silanization, therefore creating an alkynylated GO. Secondly, the CuAAC method was used to link the alkynylated GO with the azide-modified AMP. Successful covalent immobilization of the AMP was verified by XPS, where N1s spectra deconvolution showed 3 different components, including a -CONH peak and two N-N=N peaks. Area ratio of these peaks agreed with the composition ratio of a triazole structure undeniably confirming that CuAAC occurred between the alkynylated GO and the azide modified AMP. Colony counting method was employed to assess the antibacterial properties of both pristine and AMP-modified GO against *E. coli* and *S. aureus*. There was no statistical difference between pristine GO and the blank groups (control), with pristine GO showing negligible antibacterial activity. On the other hand, the AMP-grafted GO group was able to kill 80% of both bacteria, when a concentration of 80 $\mu g.mL^{-1}$ of the composite was used. These results go against what the previous works here presented showed where GO by itself had bacterial activity, although recognizably less than when it is modified with an AMP.

As shown, CuAAC "click" reaction represents an alternative to the more traditional and used approach of activating GO's carboxyl groups via EDC/NHS coupling chemistry Like EDC/NHS, this chemistry also allows for a synergistic effect when the AMP is conjugated with the GO but offers some relevant advantages such as like being a high-yield reaction that and generates virtually no by-products However, it is a much more complex process since it involves doing modifications to the structures of both GO and AMP due to the fact that none of them have alkyne and azide functional groups.

4.2.3 - Michael addition reaction

The Michael reaction corresponds to the addition of a nucleophile (Michael donor) to a α,ß-unsaturated carbonyl compound (enones), under basic conditions (Figure 2.16). Enones consists of an alkene conjugated to a ketone. Since enones (Michael acceptor) are electrophilic at the carbonyl carbon, they draw electrons from the alkene groups, making it prone to attacks by nucleophiles in nucleophilic conjugate addition [132].

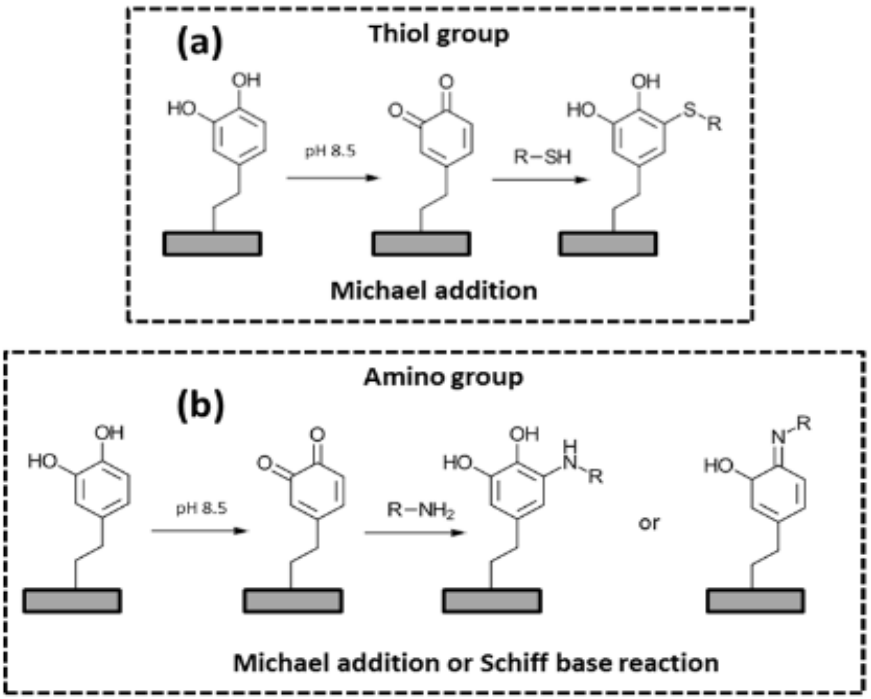

Figure 2.16 - Immobilization of biomolecules containing thiol (a) and amino (b) groups onto dopamine via Michael addition or Schiff base reaction. Adapted from [133].

Chen *et al*. reported the use of this chemistry to immobilize an AMP onto rGO, creating a new biomaterial for photothermal therapy applied to breast cancer cells. Chen´s group synthesized a nanocomposite comprised of polydopamine (pDA)-modified rGO conjugated with the pleurocidin NRC-03 AMP (known for having cytotoxic effects against breast cancer cells). Polydopamine was used to enhance near-infrared light absorbance of the composite [123]. In this case, conjugation of the AMP started with the reduction of GO by the pDA. For this effect, dopamine hydrochloride was added to GO in a Tris-HCl solution (pH = 8.5) and underwent a self-polymerization process to create a multifunctional pDA. During this process a continuous coating layer is created via the strong binding affinity of the catechol functional groups. This allow dopamine to act as both reducing agent for GO and capping agent to decorate the newly formed rGO [134]. The pDA on the pDA-rGO platform has oxygen functional groups (hydroxides) that can be used for additional functionalization, including conjugation with AMPs. Hence, the pDA-rGO, aqueous AMP solution and Tris-HCl (pH = 8.5) were mixed and stirred [123]. Since pDA´s catechol groups can be oxidized into their corresponding quinones under basic conditions, nucleophiles such as the amino groups from NCR-03 AMP are able to react with them via Michael addition reaction [133]. If the AMP had thiol residues acting as nucleophiles the reaction would most likely occur via Michael addition and not through Schiff base reaction. FTIR

spectroscopy was conducted to confirm whether GO had been successfully functionalized with the NCR-03 peptide. Pristine GO spectrum showed strong peaks at 1780 cm^{-1}, 2850 cm^{-1} and 3000 cm^{-1} corresponding to the deformation of C=O, O-H stretching and vibration of C-H, respectively, whereas the spectrum of the functionalized GO showed the exact same peaks but with decreased intensities. The authors refer that this reduction in peak intensity in the FTIR spectra is correlated with successful functionalization of the GO with the AMP, but in our view is does not constitute enough proof that peptide is covalently linked.

This work also provides a good insight over the increased peptide resistance to proteolytic degradation after its immobilization onto GBMs [123]. AMP degradation by trypsin was assessed using matrix-assisted laser desorption ionization time-of-flight (MALDI-TOF) mass spectrometry. NCR-03 alone and NCR-03-pDA/rGO were both incubated with 2 µg of trypsin at 37 ºC for 4 and 24h. After the first 4h, cleaved fragments of the peptide were identified and total degradation was observed after the 24h when the NCR-03 was not conjugated with rGO. Contrarily, it was not possible to identify cleaved fragments of the peptide at both time points in the NCR-03-pDA/rGO sample, suggesting protection against protease degradation by rGO.

Although the previous work does not explicitly show it, covalent bonds produced by Michael addition reaction are fairly more stable than the one created when NHS is used in EDC/NHS coupling chemistry, which can be seen as an advantage when comparing both approaches [133, 134].

Chapter III: Materials and Methods

1. Materials production

1.1 – Antimicrobial Peptides

The first task of this work involved selecting the AMPs most adequate for the aim application. The AMPs should be highly efficient against *Staphylococcus epidermidis* but also have broad spectrum activity. They should be short in length with a maximum of 20 mers,so it's scale-up in the future is cost-effective, include aromatic amino acids, as these facilitate the interaction of AMPs with bacterial membrane [95]. Lastly, their mode of action towards the bacteria should involve the target the cell's membrane.

Two AMPs were selected based on these requirements. The first one was KR-12 (mers: 12; amino acid sequence: KRIVQRIKDFLR; MW: 1570.98 u; isoelectric point: 12.21; net charge at pH 7: 4) [135], a fragment of the human cathelicidin peptide LL-37, one of the most studied AMPs known for its broad spectrum and immunomodulatory activities [135]. This peptide was bought from Genscript. The second AMP selected was Dhvar5 (mers: 14; amino acid sequence: LLLFLLKKRKKRKY; MW: 1847.38 u; isoelectric point: 11.64; net charge at pH 7: 7), an AMP derived from the histatin family Dh-5 with an N- to C-terminal amphipathicity [136], known for a broad spectrum of activity, including antibiotic-resistant bacteria, and already proven to be active while immobilized [136]. Dhvar5 was kindly provided by POPUP peptide synthesis facility at Faculty of Sciences of the University of Porto.

1.2 – Preparation of Antimicrobial Peptides aliquots

AMPs aliquots were made to allow a more accurate management of the peptide's stock and long-term stability. A schematic representation of the protocol is provided in Figure 3.1. Briefly, 1.2 mL of sterile-filtered 0.1M acetic acid was added to 12 mg of AMP and the solution was sonicated in an ultrasound bath (Bandelin™) for 1 minute. Next, the total volume of peptide solution was divided by the desired number of aliquots and the eppendorfs were frozen at -80 ºC for 15 minutes. After, the eppendorf's caps were cut with a sterile scissor and 0.22 µm MontaMil nylon filters were tape-glued to the top end. The eppendorfs were frozen again at -80 ºC for 30 minutes. Then, they were quickly transferred to an eppendorf support and taken

to the freeze dryer (- 80 ºC) to lyophilize overnight. The next day, the eppendorfs were closed and stored at -20 ºC until needed.

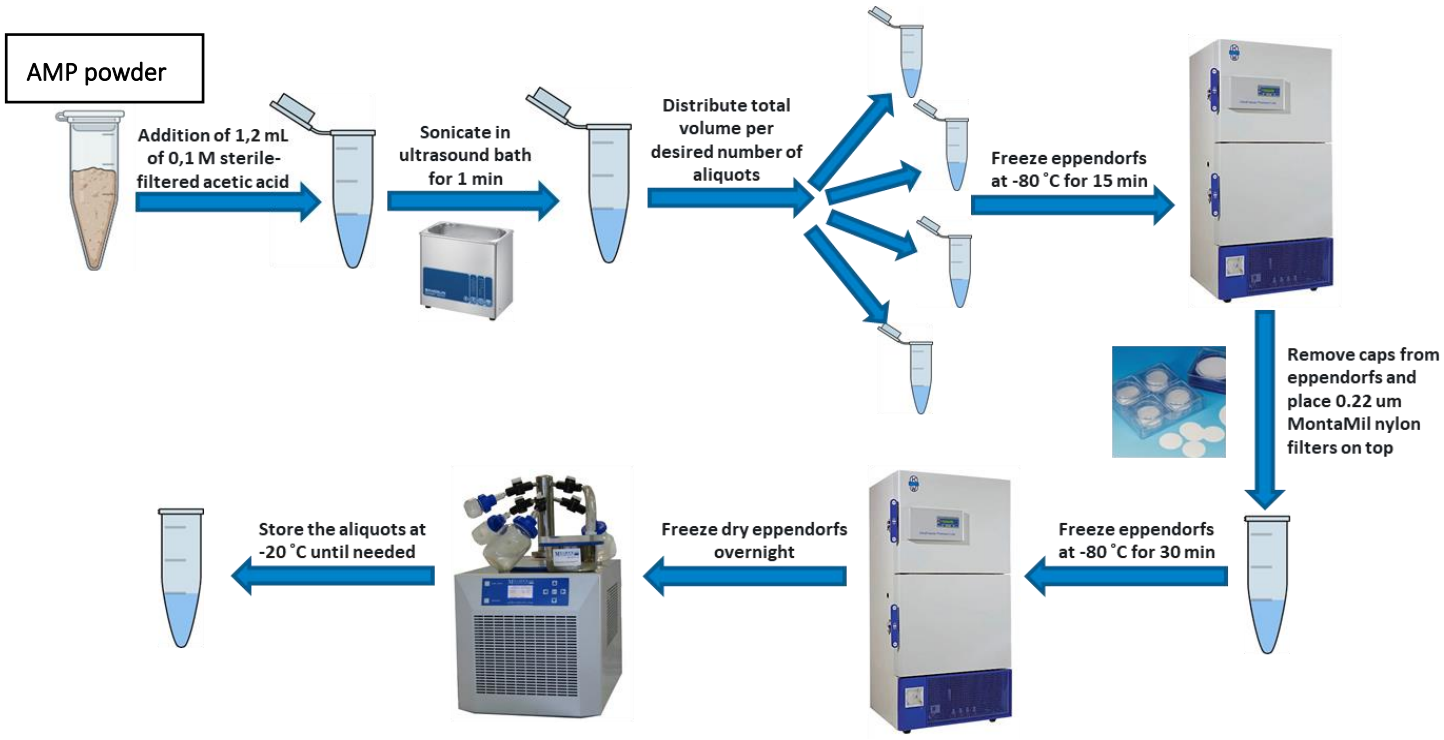

Figure 3.1 - Schematic representation of antimicrobial peptides (AMPs) aliquots preparation protocol.

1.3 - Graphene Oxide production

For this work, GO was the chosen GBM to be conjugated with the AMPs due to the presence of oxygen functional species, which offers more possibilities in terms of conjugation strategies, and also its reported antimicrobial properties [72]. Carbon graphite micro powder (99% purity and a diameter that ranged from 7 to 11 µm), which is the starting material for GO production, was purchased from American Elements, Los Angeles, USA.

GO preparation was done according to the modified Hummer's method as previously described (Figure 3.2) [11]. In brief, 8 g of graphite was added to a mixture of 320 mL of H_2SO_4 (VWR, Germany) and 80 mL of H_3PO_4 (Chem-Lab, Belgium) (4:1 ratio). This mixture was then stirred at room temperature and cooled to 0 ºC, before gradually adding 48 g of $KMnO_4$ (JMGS, Portugal). The reaction was allowed to go on at 35 ºC until the solution gained a green colour and was then stirred for 2h. After, the mixture was cooled again to 0 ºC and 1200 mL of distilled water was added. At this point, the greenish coloured mixture became brown. H_2O_2 was then added to eliminate excess $KMnO_4$ until there was no more oxygen to be released. After overnight resting, the obtained product was repeatedly centrifuged at 4000 rpm for 20 minutes, until the washing water pH was equal to dH_2O pH of 7, to ensure the removal of acidic materials or contaminants. This was followed by sonicating the solution in an ultrasonic bath for 6 hours to exfoliate the oxidized graphite into GO. GO was stored at a final concentration of 1.4 mg/mL. Whenever used, the GO suspension would be sonicated for about 20 minutes.

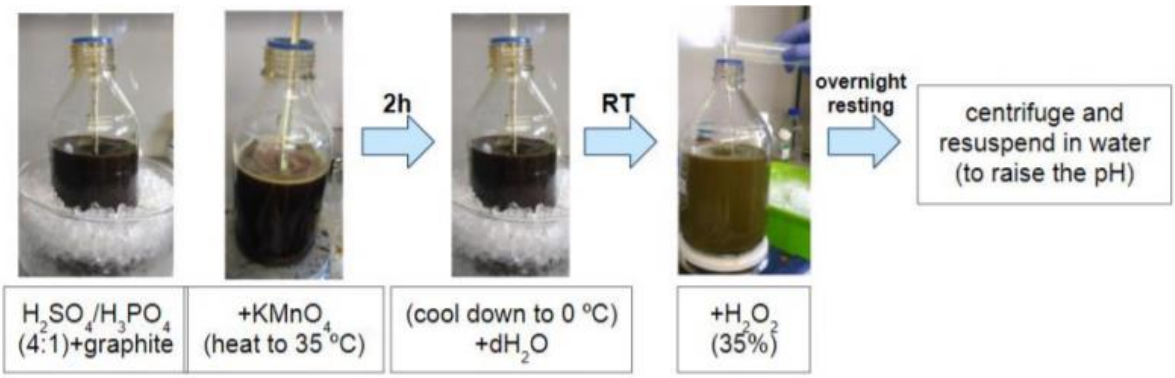

Figure 3.2 – Photographs of different stages of the Modified Hummer's Method for Graphene oxide (GO) production. Adapted from [137].

1.4 - Adsorption of the AMPs Dhvar5 and Kr-12 AMPs to GO

For the adsorption optimization of AMP to GO, 3 different weight ratios of Dhvar5 or KR-12 to GO (0.6, 0.3, 0.15 w/v) were tested, having GO as control (GO that underwent the entire conjugation process without the addition the Dhvar5). First, GO suspension (1.4 mg/mL) was centrifuged (Spectrafuge™) at 14000 rpm for 15 min and its concentration was adjusted to 1 mg/mL in phosphate-citrate buffer at pH = 7.5. Afterwards, the GO suspension was sonicated for 15 min. The mixtures of GO/AMP were prepared in the same phosphate-citrate buffer and were left to incubate under gentle stirring at 37 ºC for 24h. The GO and adsorbed AMP/GO a(AMP-GO) conjugates were rinsed twice with phosphate-citrate buffer and once with deionized water, centrifuged (14000 rpm for 15 min) and then resuspended in 50 µL of deionized water. A schematic representation of the AMP adsorption protocol is provided in Figure 3.3.

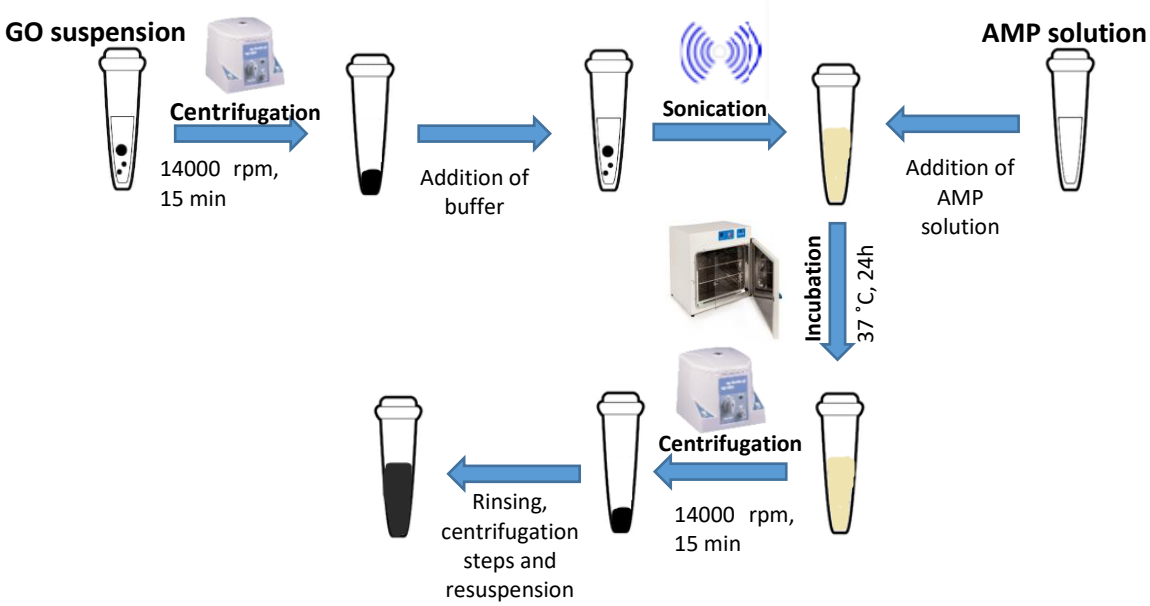

Figure 3.3- Schematic representation of the procedure for the adsorption process of Antimicrobial peptides (AMPs) onto Graphene oxide (GO).

1.5 – Covalent binding of Dhvar5 to GO via EDC/NHS coupling chemistry

Dhvar5 and GO were covalently linked using EDC/NHS coupling chemistry.

Firstly, 0.2 M 1-ethyl-3-(3-dimethylaminopropyl)carbodiimide (EDC, Sigma-Aldrich) and 0.2 M N-hydroxysuccinimide (NHS, Sigma-Aldrich) solutions were prepared using a 0.05 M 2-(N-morpholino)ethanesulfonic acid (MES; Sigma-Aldrich)) buffer at pH 6.0. After, 3 mL of GO (1mg/mL in deionized water), 72 µL of EDC solution and 720 µL of NHS solution were mixed and left to incubate at room temperature for 2h at 80 rpm. Excess EDC and NHS were removed by washing 3 times with PBS buffer pH 7.4 and GO concentration was adjusted to 62.5 µg/mL in ddH_2O. Subsequently, different amounts of Dhvar5 solution (62.5 µg/mL) were added to the now activated GO to obtain the 0.6, 0.3 and 0.15 w/v weight ratios of Dhvar5 to GO. The mixtures were left to incubate at 4 ºC for 24h at 80 rpm. After incubation period the mixtures were washed 3 times with deionized water and resuspended in 1 mL of deionized water. A schematic representation of the conjugation procedure is depicted in Figure 3.4.

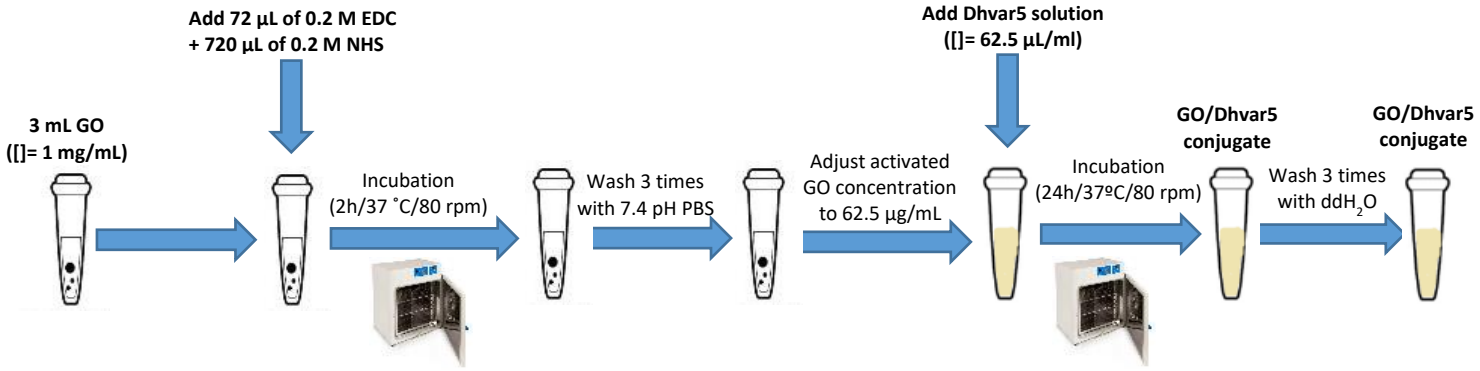

Figure 3.4 – Schematic representation of Graphene Oxide (GO) and Dhvar5 conjugation via EDC/NHS coupling chemistry.

2. Materials characterization

2.1 – GO and AMP-GO conjugates characterization

2.1.1 - X-Ray Photoelectron Spectroscopy (XPS) Analysis

Chemical composition of GO and AMP-GO conjugates was investigated by XPS analysis. To ease the characterization of AMP-GO conjugates by XPS, thin films were produced. The different suspensions of AMP-GO conjugates were spread onto 9 mm round pre-washed glass coverslips and left to dry. After, the AMP-GO coated coverslips were stored in sealed plastic petri dishes, saturated with N_2 to prevent oxidative reactions, until characterization. XPS measurements were performed at Centro de Materiais da Universidade do Porto (CEMUP, Porto, Portugal) using a Kratos Axis Ultra HSA (Kratos Analytical, UK) equipment with a monochromatic Al X-ray source operating at 15 kV (90 W). The survey spectra were acquired with a pass energy of 80 eV, with a 1 eV step size and 200 ms of dwell time. C *1s* and O *1s* high-resolution spectra were acquired with a pass energy of 20 eV, with a 0.1 eV step size and 1000 ms of dwell time.

Spectra were processed and deconvoluted using CasaXPS software (Casa Software Ltd, UK) version 2.3.18PR1.0. In order to correct the contribution of electric charge effect, all the peaks were calibrated by setting the binding energy of the C *1s* peak to 284.6 eV. The high-resolution spectra were deconvoluted using a Shirley background subtraction and Gaussian-Lorentzian functions to fit all identified functional groups. National Institute of Standards and Technology (NIST) surface database was used to constrain the binding energies of the peaks of the identified functionalities according the following data:

- C-C and C=C: 284.5 – 284.6 eV
- C-O: 285.5 – 286.7 eV (C *1s*);
- C=O: 286.8 – 287.8 eV (C *1s*);
- O-C=O: 288.6 – 290.0 eV (C *1s*);

3. Antibacterial effect assessment

3.1 – Bacteria strain and growth conditions

Staphylococcus epidermidis (ATCC 35984) was used to evaluate the antibacterial activity. The bacteria were grown in Trypticase Soy Agar (TSA) (Merck) overnight at 37 ºC.

To prepare the inoculum, two to three colonies were inoculated in 5 mL of filtered (0.22 µm) Trypticase of Soy Broth (TSB) (Merck) and were incubated overnight in an orbital shaker oven (Raypa) (150 rpm at 37 ºC). In the following day, the culture was centrifuged for 10 minutes at 2700 rpm and the resulting pellet was washed with 5 mL of TSB (centrifugation and washing steps were repeated three times), and inoculum was adjusted to obtain a concentration of 2 x 10^5 CFUs/mL in TSB by measuring the optical density at a wavelength of 600 nm (OD_{600}). Serial dilutions of the bacterial inoculum were plated on agar and incubated at 37ºC for 24h, as to confirm if the concentration had been correctly adjusted.

3.2 - Minimal Inhibitory Concentration (MIC) assay of AMPs

MIC of the selected AMPs was determined by microtiter broth dilution method [138]. Bacterial inoculum was prepared as explained in section 3.1. Next, 100 µL of the bacterial inoculum were added to each well in the 96 well microtiter plate (COSTAR®), which had been previously filled with 11 µL of serial dilutions of the tested AMPs. These peptide dilutions (400 – 0.25 µg/mL) were prepared at an initial concentration 10 times higher than the intended one, as to consider the 1:10 dilution in the microtiter plate. Additionally, several wells were either filled with just bacterial inoculum (positive control) or with TSB (growth medium sterility control). The microtiter plates were incubated at 37ºC for 24h. MIC was determined as the smallest AMP concentration that displayed no visible bacterial growth.

3.3 - Minimal Bactericidal Concentration assay (MBC) of AMPs

Minimal Bactericidal Concentration (MBCs) were determined by plating on TSA 10 µL of serial dilutions from the wells of the MIC microtiter plate where no visible bacterial growth was observed (starting from the well of the determined MIC value and the following two concentrations of AMP). After incubating for 24h at 37ºC, the MBC was determined as the concentration where no growth was observed. MIC and MBC determination is represented in Figure 3.5.

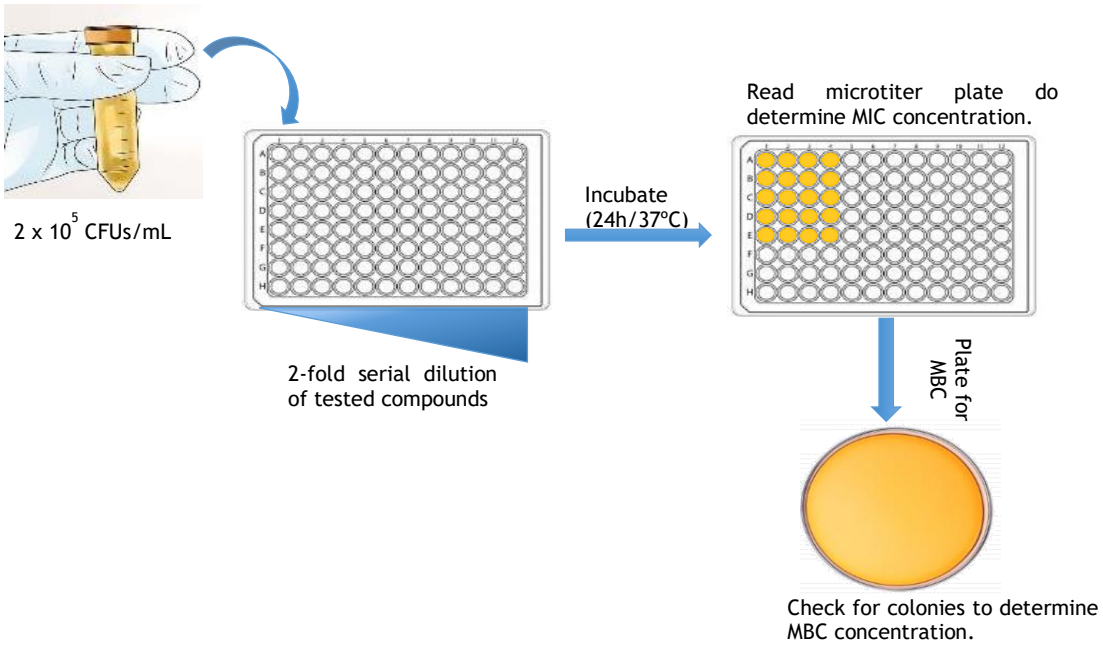

Figure 3.5 – Schematic representation of minimal inhibitory concentration (MIC) and minimal bactericidal concentration (MBC) assay.

3.3 – GO and AMP-GO conjugates antimicrobial activity assessment

GO is black, it does not allow for clear visualization of the bacterial pellet. As such, an additional test (resazurin assay) was done to confirm the obtained MIC value. Resazurin is a non-fluorescent dye that is reduced into the strongly-fluorescent dye resofurin by mitochondrial reductase of living cells that are metabolically active. MIC and MBC determination of GO (concentration range from 1.95 µg/mL to 1000 µg/mL) and AMP-GO conjugates was performed by broth dilution method, as explained in the above section (Figure 3.5). For this, at the 21st hour of the incubation period, 20 µL of resazurin was added to each well to assess the metabolic activity of *S. epidermidis* cells. The microtiter plate was left to incubate for three more hours. Then, the content of each well was transferred to a 96-well black plate so that the relative fluorescence units (RFUs) of the medium could be measured by a fluorimeter in order to determine the metabolic activity of bacteria (Figure 3.6).

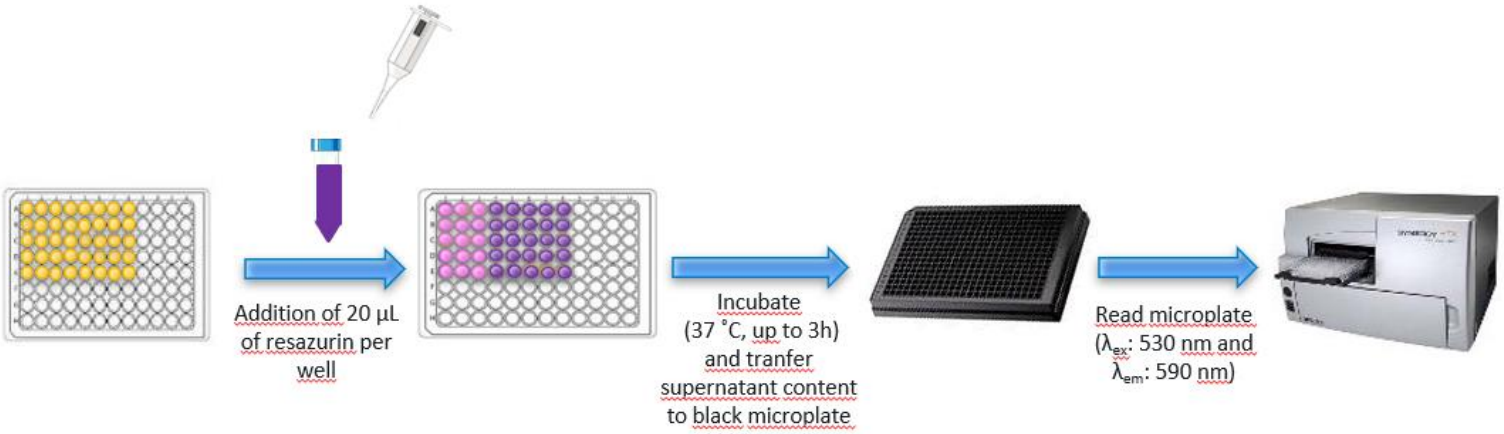

Figure 3.6 – Schematic representation for the determination of metabolic activity by resazurin assay at the end of the Minimum Inhibitory Concentration (MIC) assay.

Chapter IV: Results and Discussion

1. Antimicrobial Peptides

1.1 – Antimicrobial activity

The antimicrobial activity of the Antimicrobial peptides (AMPs) against *S. epidermidis* was assessed by minimal inhibitory concentration (MIC) (table 4.1). Dhvar5 inhibited bacteria growth starting from a concentration as low as 2 μg/mL, while KR-12 only achieved the same effect at a concentration of 100 μg/mL.

Additionally, minimal bactericidal concentration (MBC) was also determined for both peptides. The action of both AMPs was considered to be bactericidal (causes bacteria death, and not only inhibits their growth) as the MIC/MBC reported was below 3 [139].

Table 4.1- Antimicrobial activity of AMPs obtained by MIC and MBC assays.

AMP	MIC, μg/mL	MBC, μg/mL	MBC/MIC	Activity
KR-12	100	100	1	Bactericidal
Dhvar5	2	2	1	Bactericidal

As seen by the results shown in the table above, Dhvar5 is much more effective against *S. epidermidis* ATCC 35984 when compared with KR-12, since a much lower MIC and MBC value (2 μg/mL) were obtained when compared with the 100 μg/mL obtained with KR-12. Dhvar5 MIC value was in conformity with other reported studies, although we obtained a lower MBC value (2 μg/mL instead of 162 μg/mL) [140]. The results obtained with KR-12 were somewhat surprising since lower MIC and MBC values (25 – 50 μg/mL) have been described in literature using this same AMP against *S. epidermidis* [139, 141]. These differences may be related to differences on the adopted protocols, and strains of bacteria used.

2. Graphene Oxide

2.1 – Chemical characterization

Successful oxidation of graphite using Modified Hummer's Method (MHM) was verified by X-Ray Photoelectron Spectroscopy (XPS) analysis (Table 4.2).

Table 4.2 –Atomic percentages (at %) of the Carbon 1s and Oxygen 1s of the produced GO and commercially available graphite (published by Pinto *et. al* (2013)).

Element	at. % in Gt*	at. % in GO
C 1s	92	71.6
O 1s	8	28.4

XPS analysis showed that the atomic percentage of carbon in the produced GO is 71.6% and 28.4% for oxygen (Table 4.2), confirming that the graphite had been oxidized since it typically has a much lower percentage of oxygen in its structure(8% of O 1s was found in commercial pristine graphite by Pinto *et al*. [142]). The atomic percentage of oxygen in our GO is close to 30%, which is in accordance to what was expected for this material after oxidation via MHM [143].

Peak deconvolution of the GO C 1s peak (Figure 4.1), showed that C-O groups are the most prevalent oxygen-containing functional groups on the GO structure with an atomic percentage of 43.82 %. These groups appear on the basal planes of GO sheets, which have a much higher surface area in comparison to the GO sheets' edges, so it is expected for them to be the oxygen functional group with higher atomic percentage [144]. Both C=O and O-C=O groups have much lower atomic percentages (4.7 and 1.7, respectively). These values were also expected as both these groups appear on GO edges [144]. Overall, XPS analysis showed that GO was successfully oxidized from graphite with the introduction of the expected oxygenated groups after performing MHM.

A

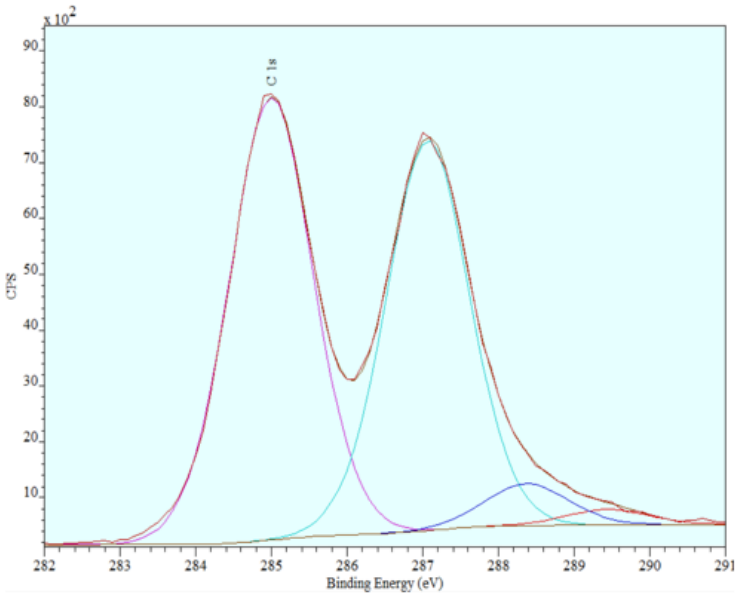

B

Chemical group	Binding energy (eV)	at. %
C=C / C-C	285	49.7
C-O	287.1	43.8
C=O	288.4	4.7
O-C=O	289.5	1.7

Figure 4.1 – A: Deconvoluted Carbon 1s high-resolution spectrum of Graphene Oxide (GO); B: Atomic percentages of the chemical groups that resulted from C 1s spectra fitting.

2.2 – Antimicrobial activity assessment

Since GBMs are known for having antimicrobial properties, the antimicrobial potential of GO was assessed by determining the MIC and MBC values against *S. epidermidis*, as well as the impact of this material on the metabolic activity of this specific bacteria. MIC was determined to be 62.5 µg/mL, but no MBC value was attained. Both 62.5, 125 and 250 µg/mL concentrations of GO (3 times higher than MIC value), allowed bacteria growth on the agar plates after the incubation period, which suggests that GO is only bacteriostatic (as proved by the MIC) and not bactericidal against this strain of *S. epidermidis*.

GO antimicrobial impact on the metabolic activity of *S. epidermidis* also assessed by resazurin assay, which measures the metabolic activity of living cells. Resazurin assay results are reported in figure 4.2. It is clear that there is a decrease in metabolically active cells when a concentration of GO of 62.5 µg/mL (MIC value) or higher is used, with only 36% or less of the existing bacteria cells being metabolically active. By lowering the concentrations of GO there are smaller decreases in metabolic activity reduction until it surpasses the metabolic activity of bacteria that were not even exposed to GO. Gupta *et. al* have reported the antibacterial activity of free GO against *S. epidermidis* [145]. Although the antibacterial activity assessment was not done by MIC assays nor resazurin assay, it showed that GO was able to inhibit the growth of *S. epidermidis* at 100 µg/mL, which is actually higher than the value that we obtained (62.5 µg/mL).

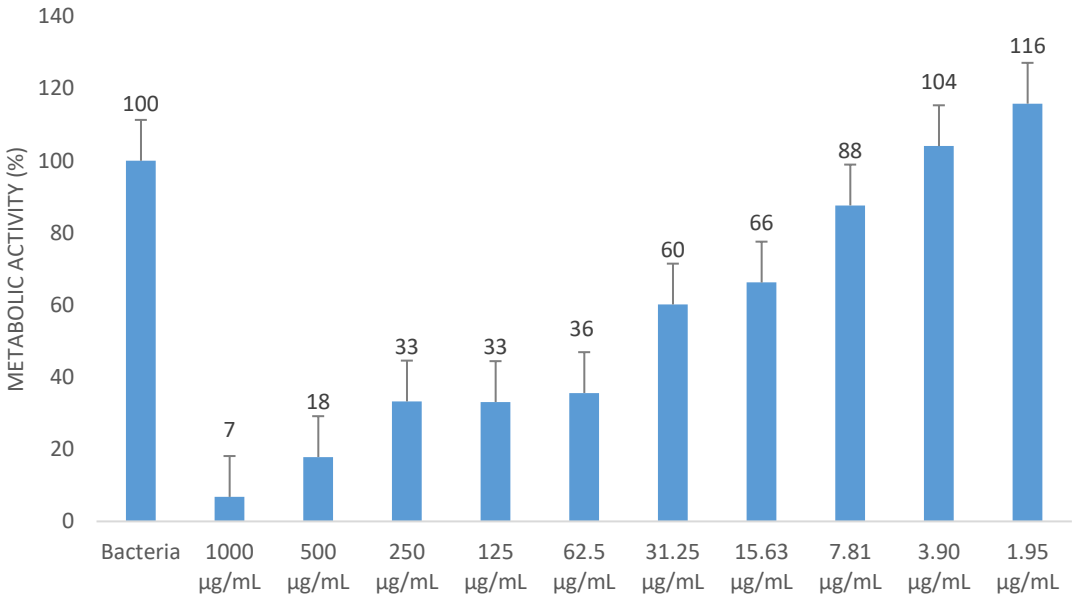

Figure 4.2 - Metabolic activity of S. epidermidis after 24h of incubation with different concentrations of Graphene oxide (GO).

3. AMP-GO conjugates

3.1 – Adsorption of KR-12 and Dhvar5 onto GO

Adsorption was the first strategy chosen to conjugate the AMPs with GO due simplicity of process and possibility of peptide release over time, so that they could work was eluting antibacterial agents.

Adsorption of the AMPs onto the GO was first done using phosphate-citrate buffer at pH 7. The suspensions of GO and of the assayed weight ratios of KR-12 to GO (0.6, 0.3, 0.15) can be seen in Figure 4.3, revealing that the addition of the AMP to the GO suspensions lead to an agglomeration between the GO particles and the peptide. A possible explanation could be the disparity in the net charges, as GO is negative and Dhvar5 has a net charge of +7 at pH 7. For this reason, we decided to do the adsorption process using different solvents (eg., dH_2O) at lower pH values, namely pH 5,to try to reduce the difference in net charge between GO and AMPs, but there were no visible alterations to this behaviour.

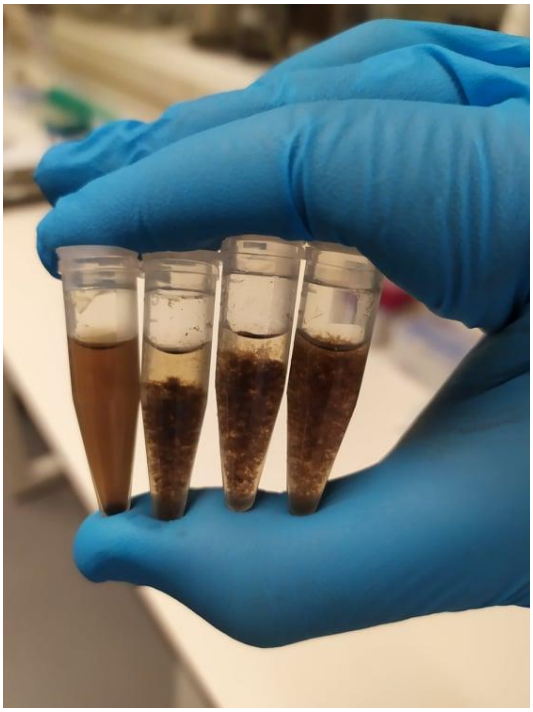

Figure 4.3 – Suspensions of Graphene oxide (GO) and KR-12-GO conjugates. From left to right: GO; 0.15 KR-12-GO; 0.3 KR-12-GO and 0.6 KR-12-GO.

3.2 - XPS analysis of AMP-GO conjugates obtained through adsorption

XPS was used to quantify the atomic composition of each sample, identify the presence of nitrogen in AMP-GO conjugates obtained through adsorption (a(AMP-GO)) (which would be indicative of AMP adsorption onto GO).

The production of GO film (control group), the 0.15 and 0.3 weight ratios of KR-12-GO conjugates films and the 0.15 weight ratio of Dhvar5-GO conjugate film on the glass coverslips was successful, allowing its analysis by XPS. The other conditions that contained higher amount of AMP, produced dispersed aggregates not an uniform film. In this way, XPS analysis was hindered since it was not possible to correctly align the x-ray beam with the crumbs. The produced films with control GO and different weight ratios of a(AMP-GO) conjugates (0.6, 0.3, 0.15) are presented in Figure 4.4.

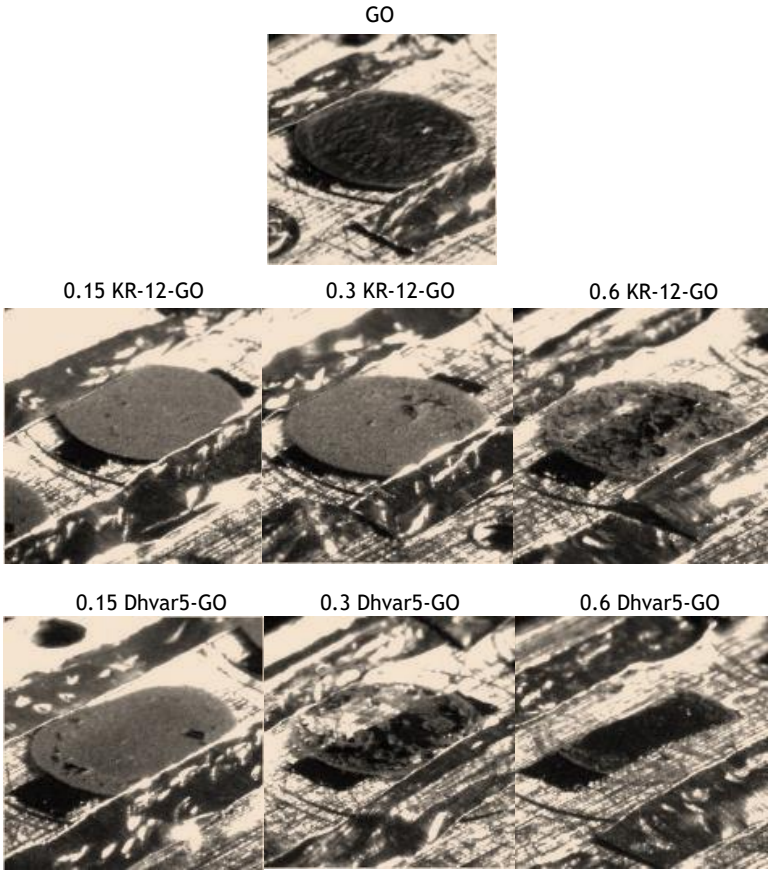

Figure 4.4 - Photograph of the preparation of the produced films for X-ray Photoelectron Spectroscopy (XPS) analysis.

The XPS survey spectra of the analysed samples shown in Figure 4.5 suggest that all samples possess a high level of chemical purity, since no contaminants were observed, with the exception of sodium (Na), which can be attributed to the use of phosphate-citrate buffer during the conjugation process, that was not fully removed even after the successive rinsing steps.. Contributions of the expected chemical elements such as the *1s* electron of carbon (C *1s*) and oxygen (O *1s*) for the GO sample and the *1s* electron of carbon (C *1s*), oxygen (O *1s*) and nitrogen (N *1s*) for the samples with conjugated AMP were observed (Figure 4.5). These results suggest

that the KR-12 and Dhvar5 conjugation with GO via adsorption was successful, as the appearance of the N *1s* peak can be assigned to amino acids. The relative atomic percentages of the chemical elements present on the surface of the analysed samples can be seen in Table 4.3. The increase in nitrogen concentration from the 0.15 KR-12-GO to the 0.3 KR-12-GO sample further supports that the AMP was conjugated with GO, as adding a higher amount of AMP to the suspension would theoretically lead to a higher nitrogen atomic percentage. Some reported studies have also used these variations in the atomic percentage of nitrogen confirm the success of the conjugation process between GO and AMPs [119, 122].

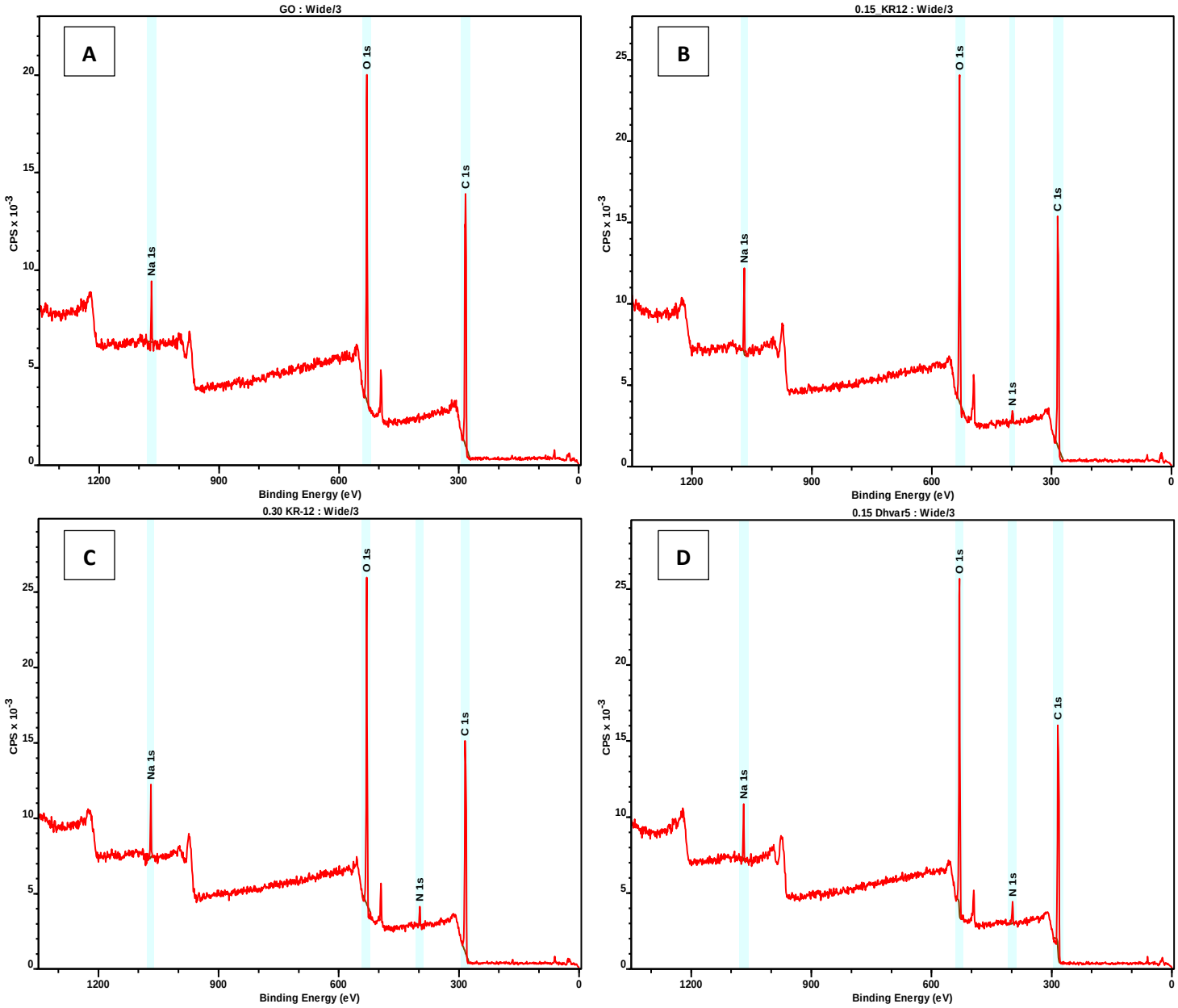

Figure 4.5 - X-ray Photoelectron Spectroscopy (XPS) survey spectra of GO (A), 0.15 KR-12-GO (B), 0.30 Kr-12-GO (C) and 0.15 Dhvar5-GO (D) conjugates. Blue areas represent the peaks' backgrounds of Sodium (Na 1s), oxygen (O 1s), nitrogen (N 1s) and carbon (C 1s), from left to right.

Table 4.3 – Relative atomic percentages of the elements present on the surface of the Graphene oxide (GO) and AMPs-GO conjugates.

Carriers	C 1s (%)	O 1s (%)	N 1s (%)
GO	72.2	27.8	-
0.15 KR-12-GO	69.0	30.0	1.4
0.30 KR-12-GO	69.2	28.5	2.3
0.15 Dhvar5-GO	69.9	27.8	2.3

3.3 – Antimicrobial activity of a(Dhvar5-GO) conjugates

We investigated the impact on the antimicrobial properties of a(Dhvar5-GO) conjugates since the MIC value for both Dhvar5 and GO against *S.epidermidis* had already been determined (2 µg/mL and 62,5 µg/mL, respectively) The same test was not performed with the KR-12 AMP as it had a much higher MIC value (100 µg/mL) when compared with Dhvar5.

As can be observed on Figure 4.6, a MIC value was not obtained for the a(Dhvar5-GO) conjugates, independently of the pH of the solvent used during conjugation, which suggests that the conjugation process might be hindering the natural antimicrobial properties of both Dhvar5 and GO. Results show that both GO and 0 control groups (GO without any treatment and GO that underwent the entire conjugation process but without adding the Dhvar5, respectively) cause a reduction of the metabolic activity, but the same is not observed when the Dhvar5 is adsorbed to the GO. In fact, it is possible to observe in all tested solvents (phosphate-citrate buffer and dH_2O, that the suspensions with higher amount of Dhvar5 (higher weight ratios) were the ones with smaller reductions in the metabolic activity of *S. epidermidis*. These findings seem to suggest that the adsorption process leads to the loss of the antimicrobial properties of both Dhvar5 and GO. As already mentioned, a possible explanation for these results may be the differences in the net charge between the highly cationic Dhvar5 and the negatively charged GO, which might be causing them to agglomerate in such a way that do not allow them to fight the bacterial cells. This same aglomeration effect was reported by Filina *et al*. when conjugating the AMP nisin with GO, which lead to loss of antimicrobial effectiveness, although the data was not shown [119].

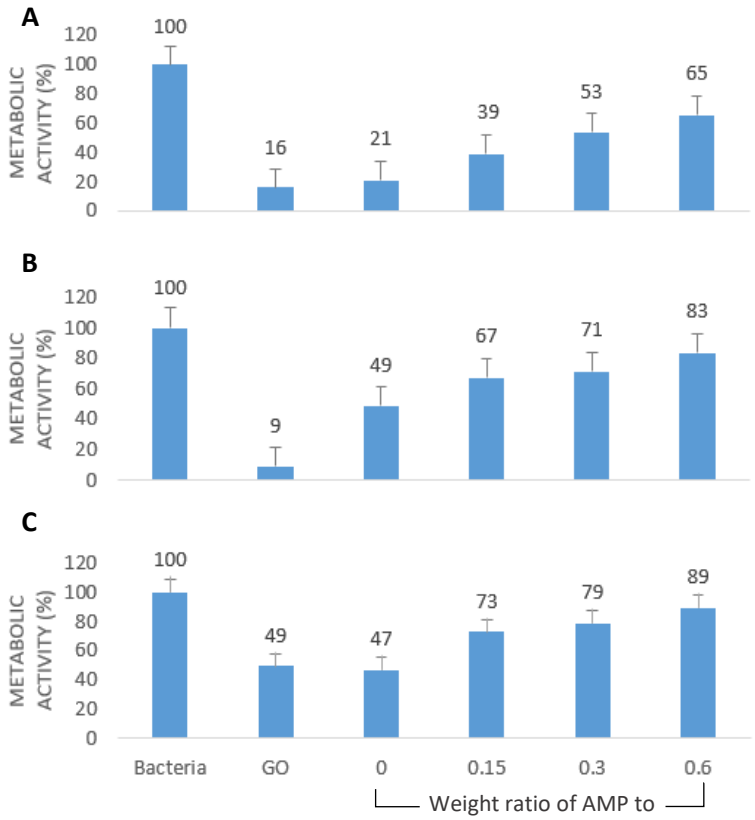

Figure 4.6 - Metabolic activity of S. epidermidis after 24h of incubation with 62.5 µg/mL of Dhvar5 conjugated GO at different weight ratios, in different solvents: (A) pH 7.5 phosphate-citrate buffer, (B) pH 7.5 ddH_2O and (C) pH 5.0 ddH_2O.

3.4 - Antimicrobial activity of Dhvar5 covalently linked GO

Unlike the a(Dhvar5-GO) conjugates, XPS characterization of the Dhvar5 covalently linked GO conjugates was not possible to perform due to the effects of the COVID-19 pandemic. Nevertheless, it was decided to indirectly evaluate the immobilization process by evaluating the antimicrobial properties of the obtained conjugates after EDC/NHS protocol.

Since adsorbing Dhvar5 to the surface of the GO did not enhanced their antimicrobial properties against *S. epidermidis*, a different approach was followed. Therefore, EDC/NHS chemistry was applied to covalently bind Dhvar5 (amine groups) to GO (carboxyl groups). Up this point, EDC/NHS coupling chemistry has been the most frequently explored approach concerning the functionalization of GO with AMPs. The success and popularity of this approach could be related to the fact that its chemistry is less complex in comparison to the other covalent approaches mentioned before in this thesis, but also because it does not require the introduction of new functional groups to GO's surface, when compared with Copper-catalysed alkyne-azide cycloaddition (CUAAC) reaction for instance.

The results obtained from the measurement of the *S. epidermidis* cell´s metabolic activity after incubation with the covalently linked Dhvar5 to GO via EDC/NHS coupling chemistry are presented in Figure 4.7. Similarly to the non-covalently linked conjugates experiment, GO and 0 control groups show a great reduction in the metabolic activity, but as soon as we start

incorporating Dhvar5 into the GO suspension (0.15, 0.3 and 0.6 weight ratios) there is a decrease in the reduction of the metabolic activity of about 30%. Additionally, no MIC or MBC was achieved.

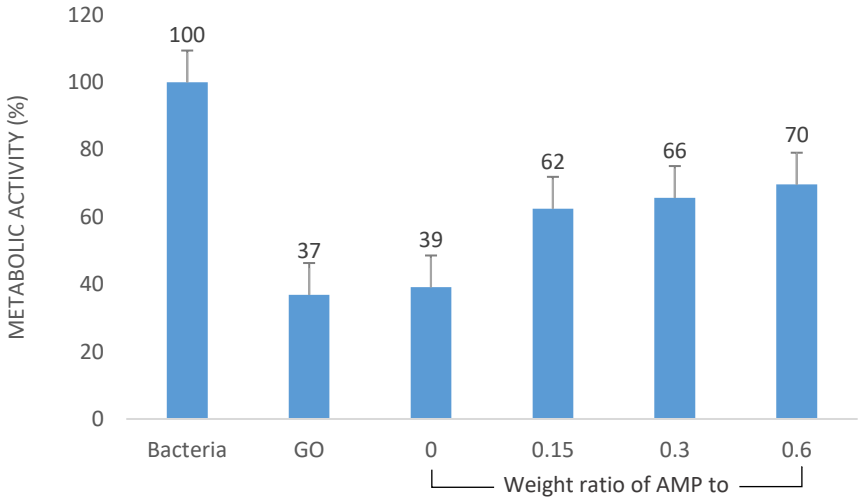

Figure 4.7 - Metabolic activity of S. epidermidis after 24h of incubation with 62.5 µg/mL of Dhvar5 conjugated GO via EDC/NHS coupling chemistry at different weight ratios.

A possible explanation for these findings could be the possibility of adsorption still occurring between the Dhvar5 and the surface of GO due to pH used in the EDC/NHS protocol, which also favours the adsorption process. This could hinder the antimicrobial ability of the peptides that were covalently kinked, leading to similar results as the ones reported in the antimicrobial activity section of the adsorbed Dhvar5-GO conjugates.

These results were not expected since we were hoping that by having Dhvar5 immobilized onto GO, they could produce a synergetic effect against the bacterial cells, as reported by some groups that also used EDC/NHS coupling chemistry to conjugate AMPs with GO [117, 118, 120]. The explanation put forward in these cases was that GO was able to hold down bacteria by a mechanical wrapping process, causing stress and physically damaging cell membranes, and further enabling electrostatic binding between the AMP and the bacteria's negatively charged membrane [118]. Nisin and Indolicidin were the conjugated AMPs in the reported studies. Both of these AMPs have a net charge of pH 7.0 of 3, while Dhvar5 has a net charge of 7 at this same pH. This could explain some adsorption phenomena even during the realization of the EDC/NHH protocol, as the much higher net charge of Dhvar5 at pH 7.4 (the pH value for the conjugation of Dhvar5 with GO in the EDC/NHS protocol) could lead to higher tendency for the peptide to agglomerate with GO, hindering both of their antimicrobial properties. Nevertheless, the results that we obtained cannot be seen as a complete surprise since the hindrance of the antimicrobial activity efficiency of immobilized AMPs has also been described in a few studies [146, 147]. Haynie et al. have shown that immobilized AMPs displayed a 50 times higher MIC when compared to soluble peptides [146], while Cho *et. al* observed a 64-fold rise of MIC values when the AMP was immobilized [147].

Chapter v: Conclusion and Future Considerations

1. Conclusion

End-stage renal disease (ESRD) affects millions of people around the world, obliging the use of either hemodialysis (HD) or peritoneal dialysis (PD) to its patients. Catheter-related infections (CRIs) represent the main cause of morbidity and second cause of mortality in people undergoing HD and PD. Moreover, a direct correlation can be found between the increase of incidence of this type of infections and the emergence of antibiotic resistant pathogens. Therefore, preventive measures, that do not use antibiotics are of utmost importance to help mitigate this serious problem.

In this work, the conjugation of Antimicrobial peptides (AMPs) with Graphene-based materials (GBMs) as a possible way of developing an antimicrobial coating that could be applied in dialysis catheters, was investigated . From the selected AMPs, Dhvar5 revealed to be much more effective against *S. epidermidis* ATCC 35984 when compared with KR-12. This was confirmed by lower MIC and MBC values (2 µg/mL) obtained with Dhvar5 then using KR-12 (100 µg/mL). Graphene oxide (GO) was successfully obtained from graphite using MHM, which was confirmed by the increase in the atomic percentage of O 1s (from 8% to 28.4%) revealed by XPS analysis. GO was selected as the GBM to be used since it offered more opportunities for functionalization due to its chemical composition but also because of its antimicrobial properties. GO elicited a MIC of 62.5 µg/mL, although no Minimal bactericidal concentration (MBC) value was found.

Non-covalent conjugation between both KR-12 and Dhvar5 with GO was achieved and confirmed by the presence of nitrogen peak by the XPS spectra, assigned to the amino acids in the AMPs. The non-covalent Dhvar5-GO conjugates did not enable to obtain either a Minimal inhibitory concentration (MIC) or MBC value, so metabolic activity measurement of *S. epidermidis* cells was performed instead. Only the Dhvar5-GO conjugates were tested since this peptide had much lower MIC and MBC values in comparison to the KR-12. The conjugation of Dhvar5 with the GO led to smaller reductions (40% to 70% less) of the metabolic activity in comparison with the control groups (only GO). Similar results were obtained after covalent functionalization of GO with Dhvar5 via EDC/NHS coupling chemistry, in terms of antimicrobial activity against *S. epidermidis,* since no MIC or MBC values were found. Dhvar5 covalently linked

to GO also displayed smaller reductions in metabolic activity (approximately 30%) in comparison to the control groups.

Globally, the strategies pursued in this thesis to conjugate the AMPs with GO did not lead to the improvement of the original antibacterial properties of both materials.

2. Future Considerations

The study developed in this thesis showed the potential of AMPs and GO against S. epidermidis, the most common bacteria responsible for the development of CRIs. However, there are still a lot of questions regarding their ability to be conjugated and what impact that might have on their antimicrobial properties.

As for future work, carboxylation of GO should be explored as this would lead to a higher percentage of carboxyl groups in the graphitic backbone, which could help while performing covalent conjugation via EDC/NHS. Solving the agglomeration problems that occur when incorporating the AMPs with GO should also be seen as a priority. The utilization of solvents at different pHs during the conjugation process very well be a strategy to overcome this.

New functionalization techniques can be pursued in order to improve the antibacterial properties of this material. CuAAC might be a suitable chemistry for this purpose as some studies have reported.

Additionally, the proteolytic degradation of the AMP while immobilized onto the GO should also be investigated, since the immobilization process should make them less vulnerable to the action of the proteases present in the serum, but very few studies have been conducted to assess this property.

Finally, the biocompability and toxicity of the AMP/GO conjugates is to be investigated as these novel biomaterials could potentially be incorporated onto dialysis catheters.

References

1. *National Kidney Foundation. Kidney Disease Quality Outcomes Initiative (K/DOQI)*. 15 December 2019]; Available from: http://www.kidney.org/professionals/kdoqi/guidelines.cfm.
2. Abbasi, M.A., G.M. Chertow, and Y.N. Hall, *End-stage renal disease.* BMJ clinical evidence, 2010. **2010**: p. 2002.
3. Liyanage, T., et al., *Worldwide access to treatment for end-stage kidney disease: a systematic review.* Lancet, 2015. **385**(9981): p. 1975-82.
4. Couser, W.G., et al., *The contribution of chronic kidney disease to the global burden of major noncommunicable diseases.* Kidney Int, 2011. **80**(12): p. 1258-70.
5. *Chapter 9: healthcare expenditures for persons with ESRD*. 2017; Available from: https://www.usrds.org/2017/view/v2_09.aspx.
6. Gahlot, R., et al., *Catheter-related bloodstream infections.* International journal of critical illness and injury science, 2014. **4**(2): p. 162-167.
7. Lata, C., et al., *Catheter-related bloodstream infection in end-stage kidney disease: a Canadian narrative review.* Canadian journal of kidney health and disease, 2016. **3**: p. 24-24.
8. Eleftheriadis, T., et al., *Infections in hemodialysis: a concise review - Part 1: bacteremia and respiratory infections.* Hippokratia, 2011. **15**(1): p. 12-17.
9. Al Wakeel, J.S., et al., *Morbidity and mortality in ESRD patients on dialysis.* Saudi J Kidney Dis Transpl, 2002. **13**(4): p. 473-7.
10. McCue, J.D., C. Hansen, and P. Gal, *Hospital charges for antibiotics.* Rev Infect Dis, 1985. **7**(5): p. 643-5.
11. Pinto, A.M., et al., *Smaller particle size and higher oxidation improves biocompatibility of graphene-based materials.* Carbon, 2016. **99**: p. 318-329.
12. Perreault, F., et al., *Antimicrobial Properties of Graphene Oxide Nanosheets: Why Size Matters.* ACS Nano, 2015. **9**(7): p. 7226-7236.
13. *End-stage renal disease*. Available from: https://www.mayoclinic.org/diseases-conditions/end-stage-renal-disease/symptoms-causes/syc-20354532.
14. Gueutin, V., G. Deray, and C. Isnard-Bagnis, *[Renal physiology].* Bull Cancer, 2012. **99**(3): p. 237-49.
15. Boima, V., *Creatinine based equations and glomerular filtration rate: interpretation and clinical relevance.* Ghana medical journal, 2016. **50**(3): p. 119-121.
16. Kalantar-Zadeh, K., et al., *Fluid retention is associated with cardiovascular mortality in patients undergoing long-term hemodialysis.* Circulation, 2009. **119**(5): p. 671-679.
17. Chartsrisak, K., et al., *Mineral metabolism and outcomes in chronic kidney disease stage 2-4 patients.* BMC nephrology, 2013. **14**: p. 14-14.
18. Iorember, F.M., *Malnutrition in Chronic Kidney Disease.* Frontiers in pediatrics, 2018. **6**: p. 161-161.

19. Becker, P.J., et al., *Consensus statement of the Academy of Nutrition and Dietetics/American Society for Parenteral and Enteral Nutrition: indicators recommended for the identification and documentation of pediatric malnutrition (undernutrition).* J Acad Nutr Diet, 2014. **114**(12): p. 1988-2000.
20. Adamson, J.W., J. Eschbach, and C.A. Finch, *The kidney and erythropoiesis.* The American Journal of Medicine, 1968. **44**(5): p. 725-733.
21. Clinic, M. *Hemodialysis*. July 23, 2019 Available from: https://www.mayoclinic.org/tests-procedures/hemodialysis/about/pac-20384824.
22. Clinic, M. *Peritoneal dialysis*. April 24, 2019; Available from: https://www.mayoclinic.org/tests-procedures/peritoneal-dialysis/about/pac-20384725.
23. *Dialysis*. Access on 05/January/2019]; Available from: https://www.msdmanuals.com/home/kidney-and-urinary-tract-disorders/dialysis/dialysis.
24. Sarnak, M.J. and B.L. Jaber, *Mortality caused by sepsis in patients with end-stage renal disease compared with the general population.* Kidney International, 2000. **58**(4): p. 1758-1764.
25. Gahlot, R., et al., *Catheter-related bloodstream infections.* International Journal of Critical Illness and Injury Science, 2014. **4**(2): p. 162-167.
26. Sarnak, M.J. and B.L. Jaber, *Mortality caused by sepsis in patients with end-stage renal disease compared with the general population.* Kidney Int, 2000. **58**(4): p. 1758-64.
27. Akoh, J.A., *Peritoneal dialysis associated infections: An update on diagnosis and management.* World journal of nephrology, 2012. **1**(4): p. 106-122.
28. Akoh, J.A., *Peritoneal dialysis associated infections: An update on diagnosis and management.* World J Nephrol, 2012. **1**(4): p. 106-22.
29. Otto, M., *Staphylococcus epidermidis--the 'accidental' pathogen.* Nat Rev Microbiol, 2009. **7**(8): p. 555-67.
30. Saising, J., et al., *Activity of gallidermin on Staphylococcus aureus and Staphylococcus epidermidis biofilms.* Antimicrobial agents and chemotherapy, 2012. **56**(11): p. 5804-5810.
31. Rupp, M.E. and G.L. Archer, *Coagulase-negative staphylococci: pathogens associated with medical progress.* Clin Infect Dis, 1994. **19**(2): p. 231-43; quiz 244-5.
32. Akoh, J., *Peritoneal dialysis associated infections: An update on diagnosis and management.* World journal of nephrology, 2012. **1**: p. 106-122.
33. Sengupta, S., M.K. Chattopadhyay, and H.-P. Grossart, *The multifaceted roles of antibiotics and antibiotic resistance in nature.* Frontiers in microbiology, 2013. **4**: p. 47-47.
34. Ventola, C.L., *The antibiotic resistance crisis: part 1: causes and threats.* P & T : a peer-reviewed journal for formulary management, 2015. **40**(4): p. 277-283.
35. Zhang, M., J. Zhao, and J. Zheng, *Molecular understanding of a potential functional link between antimicrobial and amyloid peptides.* Soft Matter, 2014. **10**(38): p. 7425-7451.
36. Jones, K.E., et al., *Global trends in emerging infectious diseases.* Nature, 2008. **451**(7181): p. 990-993.
37. *Antimicrobial Resistance: Tackling a Crisis for the Future Health and Wealth of Nations*. 2014 [cited last accessed on December 12, 2019.; Available from: http://amr-review.org/.
38. Bartlett, J.G., D.N. Gilbert, and B. Spellberg, *Seven ways to preserve the miracle of antibiotics.* Clin Infect Dis, 2013. **56**(10): p. 1445-50.
39. Abdul Gafor, A.H., et al., *Antibiogram for Haemodialysis Catheter-Related Bloodstream Infections.* International Journal of Nephrology, 2014. **2014**: p. 629459.
40. Aslam, B., et al., *Antibiotic resistance: a rundown of a global crisis.* Infection and drug resistance, 2018. **11**: p. 1645-1658.

41. An, Y.H. and R.J. Friedman, *Concise review of mechanisms of bacterial adhesion to biomaterial surfaces.* Journal of Biomedical Materials Research, 1998. **43**(3): p. 338-348.
42. Gottenbos, B., et al., *Antimicrobial effects of positively charged surfaces on adhering Gram-positive and Gram-negative bacteria.* Journal of Antimicrobial Chemotherapy, 2001. **48**(1): p. 7-13.
43. Hogt, A.H., J. Dankert, and J. Feijen, *Adhesion of coagulase-negative staphylococci to methacrylate polymers and copolymers.* J Biomed Mater Res, 1986. **20**(4): p. 533-45.
44. Chen, S., et al., *Surface hydration: Principles and applications toward low-fouling/nonfouling biomaterials.* Polymer, 2010. **51**(23): p. 5283-5293.
45. Banerjee, I., R.C. Pangule, and R.S. Kane, *Antifouling Coatings: Recent Developments in the Design of Surfaces That Prevent Fouling by Proteins, Bacteria, and Marine Organisms.* Advanced Materials, 2011. **23**(6): p. 690-718.
46. Zhang, H. and M. Chiao, *Anti-fouling Coatings of Poly(dimethylsiloxane) Devices for Biological and Biomedical Applications.* Journal of Medical and Biological Engineering, 2015. **35**(2): p. 143-155.
47. Hadjesfandiari, N., et al., *Polymer brush-based approaches for the development of infection-resistant surfaces.* Journal of Materials Chemistry B, 2014. **2**(31): p. 4968-4978.
48. Wu, J., et al., *Probing the weak interaction of proteins with neutral and zwitterionic antifouling polymers.* Acta Biomaterialia, 2014. **10**(2): p. 751-760.
49. Cheng, G., et al., *Inhibition of bacterial adhesion and biofilm formation on zwitterionic surfaces.* Biomaterials, 2007. **28**(29): p. 4192-4199.
50. Junter, G.-A., P. Thébault, and L. Lebrun, *Polysaccharide-based antibiofilm surfaces.* Acta Biomaterialia, 2016. **30**: p. 13-25.
51. Li, M., et al., *Surface Modification of Silicone with Covalently Immobilized and Crosslinked Agarose for Potential Application in the Inhibition of Infection and Omental Wrapping.* Advanced Functional Materials, 2014. **24**(11): p. 1631-1643.
52. Neoh, K.G., et al., *Surface modification strategies for combating catheter-related complications: recent advances and challenges.* Journal of Materials Chemistry B, 2017. **5**(11): p. 2045-2067.
53. Morones-Ramirez, J.R., et al., *Silver Enhances Antibiotic Activity Against Gram-Negative Bacteria.* Science Translational Medicine, 2013. **5**(190): p. 190ra81.
54. Zhang, S., et al., *Enhanced Antibacterial and Antiadhesive Activities of Silver-PTFE Nanocomposite Coating for Urinary Catheters.* ACS Biomaterials Science & Engineering, 2019. **5**(6): p. 2804-2814.
55. Wo, Y., et al., *Recent advances in thromboresistant and antimicrobial polymers for biomedical applications: just say yes to nitric oxide (NO).* Biomaterials Science, 2016. **4**(8): p. 1161-1183.
56. Tran, P., A. Hamood, and T. Reid, *Antimicrobial Coatings to Prevent Biofilm Formation on Medical Devices*. 2014. p. 175-204.
57. Raad, I., et al., *Central venous catheters coated with minocycline and rifampin for the prevention of catheter-related colonization and bloodstream infections. A randomized, double-blind trial. The Texas Medical Center Catheter Study Group.* Ann Intern Med, 1997. **127**(4): p. 267-74.
58. Schierholz, J.M., et al., *Controlled release of antibiotics from biomedical polyurethanes: morphological and structural features.* Biomaterials, 1997. **18**(12): p. 839-844.
59. Fisher, L.E., et al., *Biomaterial modification of urinary catheters with antimicrobials to give long-term broadspectrum antibiofilm activity.* Journal of Controlled Release, 2015. **202**: p. 57-64.
60. Andersson, D.I. and D. Hughes, *Microbiological effects of sublethal levels of antibiotics.* Nature Reviews Microbiology, 2014. **12**(7): p. 465-478.

61. Bagheri, M., M. Beyermann, and M. Dathe, *Immobilization Reduces the Activity of Surface-Bound Cationic Antimicrobial Peptides with No Influence upon the Activity Spectrum.* Antimicrobial Agents and Chemotherapy, 2009. **53**(3): p. 1132.
62. Muszanska, A.K., et al., *Antiadhesive Polymer Brush Coating Functionalized with Antimicrobial and RGD Peptides to Reduce Biofilm Formation and Enhance Tissue Integration.* Biomacromolecules, 2014. **15**(6): p. 2019-2026.
63. Cavallaro, A., et al., *Influence of immobilized quaternary ammonium group surface density on antimicrobial efficacy and cytotoxicity.* Biofouling, 2016. **32**(1): p. 13-24.
64. Xue, Y., H. Xiao, and Y. Zhang, *Antimicrobial polymeric materials with quaternary ammonium and phosphonium salts.* Int J Mol Sci, 2015. **16**(2): p. 3626-55.
65. Costa, F.M., et al., *Dhvar5 antimicrobial peptide (AMP) chemoselective covalent immobilization results on higher antiadherence effect than simple physical adsorption.* Biomaterials, 2015. **52**: p. 531-8.
66. Gabriel, M., et al., *Preparation of LL-37-Grafted Titanium Surfaces with Bactericidal Activity.* Bioconjugate Chemistry, 2006. **17**(2): p. 548-550.
67. Shi, Z., K.G. Neoh, and E.T. Kang, *Antibacterial and Adsorption Characteristics of Activated Carbon Functionalized with Quaternary Ammonium Moieties.* Industrial & Engineering Chemistry Research, 2007. **46**(2): p. 439-445.
68. Cen, L., K.G. Neoh, and E.T. Kang, *Surface Functionalization Technique for Conferring Antibacterial Properties to Polymeric and Cellulosic Surfaces.* Langmuir, 2003. **19**(24): p. 10295-10303.
69. Costa, F., et al., *Covalent immobilization of antimicrobial peptides (AMPs) onto biomaterial surfaces.* Acta Biomater, 2011. **7**(4): p. 1431-40.
70. An, X., et al., *Graphene Oxide Reinforced Polylactic Acid/Polyurethane Antibacterial Composites.* Journal of Nanomaterials, 2013. **2013**.
71. Borges, I., et al., *Exposure of Smaller and Oxidized Graphene on Polyurethane Surface Improves its Antimicrobial Performance.* Nanomaterials (Basel, Switzerland), 2020. **10**(2): p. 349.
72. Henriques, P.C., et al., *Fabrication and antimicrobial performance of surfaces integrating graphene-based materials.* Carbon, 2018. **132**: p. 709-732.
73. Kitko, K.E. and Q. Zhang, *Graphene-Based Nanomaterials: From Production to Integration With Modern Tools in Neuroscience.* Frontiers in Systems Neuroscience, 2019. **13**(26).
74. Mohan, V.B., et al., *Graphene-based materials and their composites: A review on production, applications and product limitations.* Composites Part B: Engineering, 2018. **142**: p. 200-220.
75. Jiang, B., et al., *Label-free glucose biosensor based on enzymatic graphene oxide-functionalized tilted fiber grating.* Sensors and Actuators B: Chemical, 2018. **254**: p. 1033-1039.
76. Qin, J., et al., *Graphene Networks Anchored with Sn@Graphene as Lithium Ion Battery Anode.* ACS Nano, 2014. **8**(2): p. 1728-1738.
77. Rao, Z., et al., *Carboxymethyl cellulose modified graphene oxide as pH-sensitive drug delivery system.* International Journal of Biological Macromolecules, 2018. **107**: p. 1184-1192.
78. Singh, V., et al., *Graphene based materials: Past, present and future.* Progress in Materials Science, 2011. **56**(8): p. 1178-1271.
79. Lee, X.J., et al., *Review on graphene and its derivatives: Synthesis methods and potential industrial implementation.* Journal of the Taiwan Institute of Chemical Engineers, 2019. **98**: p. 163-180.
80. Edwards, R.S. and K.S. Coleman, *Graphene synthesis: relationship to applications.* Nanoscale, 2013. **5**(1): p. 38-51.

81. Rowley-Neale, S.J., et al., *An overview of recent applications of reduced graphene oxide as a basis of electroanalytical sensing platforms.* Applied Materials Today, 2018. **10**: p. 218-226.
82. Dideikin, A. and A. Vul, *Graphene Oxide and Derivatives: The Place in Graphene Family.* Frontiers in Physics, 2019. **6**.
83. Azizighannad, S. and S. Mitra, *Stepwise Reduction of Graphene Oxide (GO) and Its Effects on Chemical and Colloidal Properties.* Scientific Reports, 2018. **8**(1): p. 10083.
84. Choi, J., et al., *Controlled oxidation level of reduced graphene oxides and its effect on thermoelectric properties.* Macromolecular Research, 2014. **22**(10): p. 1104-1108.
85. Shih, C.-J., et al., *Understanding the pH-Dependent Behavior of Graphene Oxide Aqueous Solutions: A Comparative Experimental and Molecular Dynamics Simulation Study.* Langmuir, 2012. **28**(1): p. 235-241.
86. Konkena, B. and S. Vasudevan, *Understanding Aqueous Dispersibility of Graphene Oxide and Reduced Graphene Oxide through pKa Measurements.* J Phys Chem Lett, 2012. **3**(7): p. 867-72.
87. Chen, J., et al., *Graphene oxide exhibits broad-spectrum antimicrobial activity against bacterial phytopathogens and fungal conidia by intertwining and membrane perturbation.* Nanoscale, 2014. **6**(3): p. 1879-89.
88. PriyaSwetha, P.D., et al., *Antimicrobial Properties of Sonochemically Treated Graphene Oxides Sheets.* Materials Today: Proceedings, 2018. **5**(8, Part 3): p. 16669-16674.
89. Kumar, P., et al., *Antibacterial Properties of Graphene-Based Nanomaterials.* Nanomaterials (Basel, Switzerland), 2019. **9**(5): p. 737.
90. Zou, X., et al., *Mechanisms of the Antimicrobial Activities of Graphene Materials.* Journal of the American Chemical Society, 2016. **138**(7): p. 2064-2077.
91. Chen, J., et al., *Antibacterial activity of graphene-modified anode on Shewanella oneidensis MR-1 biofilm in microbial fuel cell.* Journal of Power Sources, 2015. **290**: p. 80-86.
92. Krishnamoorthy, K., et al., *Antibacterial Activity of Graphene Oxide Nanosheets*. Vol. 4. 2012. 1-7.
93. Navya Rani, M., S. Ananda, and D. Rangappa, *Preparation of Reduced Graphene Oxide and Its Antibacterial Properties.* Materials Today: Proceedings, 2017. **4**(11, Part 3): p. 12300-12305.
94. Hegab, H.M., et al., *The controversial antibacterial activity of graphene-based materials.* Carbon, 2016. **105**: p. 362-376.
95. Mahlapuu, M., et al., *Antimicrobial Peptides: An Emerging Category of Therapeutic Agents.* Frontiers in cellular and infection microbiology, 2016. **6**: p. 194-194.
96. Katzenback, B.A., *Antimicrobial Peptides as Mediators of Innate Immunity in Teleosts.* Biology (Basel), 2015. **4**(4): p. 607-39.
97. Diamond, G., et al., *The roles of antimicrobial peptides in innate host defense.* Curr Pharm Des, 2009. **15**(21): p. 2377-92.
98. van 't Hof, W., et al., *Antimicrobial peptides: properties and applicability.* Biol Chem, 2001. **382**(4): p. 597-619.
99. Hancock, R.E. and G. Diamond, *The role of cationic antimicrobial peptides in innate host defences.* Trends Microbiol, 2000. **8**(9): p. 402-10.
100. Wang, J., et al., *Antimicrobial Peptides with High Proteolytic Resistance for Combating Gram-Negative Bacteria.* Journal of Medicinal Chemistry, 2019. **62**(5): p. 2286-2304.
101. Bahar, A.A. and D. Ren, *Antimicrobial peptides.* Pharmaceuticals (Basel, Switzerland), 2013. **6**(12): p. 1543-1575.
102. Huang, Y., J. Huang, and Y. Chen, *Alpha-helical cationic antimicrobial peptides: relationships of structure and function.* Protein Cell, 2010. **1**(2): p. 143-52.
103. Koehbach, J. and D.J. Craik, *The Vast Structural Diversity of Antimicrobial Peptides.* Trends in Pharmacological Sciences, 2019. **40**(7): p. 517-528.

104. Bulet, P., R. Stocklin, and L. Menin, *Anti-microbial peptides: from invertebrates to vertebrates.* Immunol Rev, 2004. **198**: p. 169-84.
105. Yeaman, M.R. and N.Y. Yount, *Mechanisms of antimicrobial peptide action and resistance.* Pharmacol Rev, 2003. **55**(1): p. 27-55.
106. Lin, T.Y. and D.B. Weibel, *Organization and function of anionic phospholipids in bacteria.* Appl Microbiol Biotechnol, 2016. **100**(10): p. 4255-67.
107. Hancock, R.E. and D.S. Chapple, *Peptide antibiotics.* Antimicrob Agents Chemother, 1999. **43**(6): p. 1317-23.
108. Zasloff, M., *Antimicrobial peptides of multicellular organisms.* Nature, 2002. **415**(6870): p. 389-95.
109. Marquette, A. and B. Bechinger, *Biophysical Investigations Elucidating the Mechanisms of Action of Antimicrobial Peptides and Their Synergism.* Biomolecules, 2018. **8**: p. 18.
110. Kumar, P., J.N. Kizhakkedathu, and S.K. Straus, *Antimicrobial Peptides: Diversity, Mechanism of Action and Strategies to Improve the Activity and Biocompatibility In Vivo.* Biomolecules, 2018. **8**(1).
111. Kumar, P., J. Kizhakkedathu, and S. Straus, *Antimicrobial Peptides: Diversity, Mechanism of Action and Strategies to Improve the Activity and Biocompatibility In Vivo.* Biomolecules, 2018. **8**.
112. Russell, S.R. and S.A. Claridge, *Peptide interfaces with graphene: an emerging intersection of analytical chemistry, theory, and materials.* Anal Bioanal Chem, 2016. **408**(11): p. 2649-58.
113. Mann, J.A. and W.R. Dichtel, *Noncovalent Functionalization of Graphene by Molecular and Polymeric Adsorbates.* The Journal of Physical Chemistry Letters, 2013. **4**(16): p. 2649-2657.
114. Georgakilas, V., et al., *Noncovalent Functionalization of Graphene and Graphene Oxide for Energy Materials, Biosensing, Catalytic, and Biomedical Applications.* Chemical Reviews, 2016. **116**(9): p. 5464-5519.
115. Mannoor, M.S., et al., *Graphene-based wireless bacteria detection on tooth enamel.* Nature Communications, 2012. **3**(1): p. 763.
116. Kim, S.N., et al., *Preferential Binding of Peptides to Graphene Edges and Planes.* Journal of the American Chemical Society, 2011. **133**(37): p. 14480-14483.
117. Kanchanapally, R., et al., *Antimicrobial peptide-conjugated graphene oxide membrane for efficient removal and effective killing of multiple drug resistant bacteria.* RSC Advances, 2015. **5**(24): p. 18881-18887.
118. Pramanik, A., et al., *Composites Composed of Polydopamine Nanoparticles, Graphene Oxide, and ε-Poly-l-lysine for Removal of Waterborne Contaminants and Eradication of Superbugs.* ACS Applied Nano Materials, 2019. **2**(6): p. 3339-3347.
119. Filina, A., et al., *Antimicrobial Hierarchically Porous Graphene Oxide Sponges for Water Treatment.* ACS Applied Bio Materials, 2019. **2**(4): p. 1578-1590.
120. Farzanegan, A., et al., *Synthesis, characterization and antifungal activity of a novel formulated nanocomposite containing Indolicidin and Graphene oxide against disseminated candidiasis.* J Mycol Med, 2018. **28**(4): p. 628-636.
121. Chen, Y., et al., *Electronic Detection of Bacteria Using Holey Reduced Graphene Oxide.* ACS Applied Materials & Interfaces, 2014. **6**(6): p. 3805-3810.
122. Shi, L., et al., *Modifying graphene oxide with short peptide via click chemistry for biomedical applications.* Applied Materials Today, 2016. **5**: p. 111-117.
123. Chen, Y.-C., et al., *Enhanced Efficient NIR Photothermal Therapy Using Pleurocidin NRC-03 Peptide-Conjugated Dopamine-Modified Reduced Graphene Oxide Nanocomposite.* ACS Omega, 2019. **4**(2): p. 3298-3305.
124. Kasprzak, A., A. Zuchowska, and M. Poplawska, *Functionalization of graphene: does the organic chemistry matter?* Beilstein Journal of Organic Chemistry, 2018. **14**: p. 2018-2026.

125. Wickramathilaka, M.P. and B.Y. Tao, *Characterization of covalent crosslinking strategies for synthesizing DNA-based bioconjugates.* Journal of Biological Engineering, 2019. **13**(1): p. 63.
126. Schoning, M.J. and A. Poghossian, *Recent advances in biologically sensitive field-effect transistors (BioFETs).* Analyst, 2002. **127**(9): p. 1137-51.
127. Cernat, A., et al., *Click chemistry on azide-functionalized graphene oxide.* Electrochemistry Communications, 2019. **98**: p. 23-27.
128. Zhu, L., et al., *On the Mechanism of Copper(I)-Catalyzed Azide–Alkyne Cycloaddition.* The Chemical Record, 2016. **16**(3): p. 1501-1517.
129. Hein, J.E. and V.V. Fokin, *Copper-catalyzed azide-alkyne cycloaddition (CuAAC) and beyond: new reactivity of copper(I) acetylides.* Chem Soc Rev, 2010. **39**(4): p. 1302-15.
130. Moses, J.E. and A.D. Moorhouse, *The growing applications of click chemistry.* Chem Soc Rev, 2007. **36**(8): p. 1249-62.
131. Liang, L. and D. Astruc, *The copper(I)-catalyzed alkyne-azide cycloaddition (CuAAC) "click" reaction and its applications. An overview.* Coordination Chemistry Reviews, 2011. **255**(23): p. 2933-2945.
132. Little, R.D., Masjedizadeh, M. R., Wallquist, O. and Mcloughlin, J. I., *The Intramolecular Michael Reaction*, in *Organic Reactions*. 2004. p. 315-552.
133. Salazar, P., M. Martín, and J. González-Mora, *Polydopamine-modified surfaces in biosensor applications*. 2016. p. 385-396.
134. Huang, N., et al., *Multifunctional Electrochemical Platforms Based on the Michael Addition/Schiff Base Reaction of Polydopamine Modified Reduced Graphene Oxide: Construction and Application.* ACS Applied Materials & Interfaces, 2015. **7**(32): p. 17935-17946.
135. Saporito, P., et al., *LL-37 fragments have antimicrobial activity against Staphylococcus epidermidis biofilms and wound healing potential in HaCaT cell line.* Journal of Peptide Science, 2018. **24**(7): p. e3080.
136. Costa, F.M.T.A., et al., *Dhvar5 antimicrobial peptide (AMP) chemoselective covalent immobilization results on higher antiadherence effect than simple physical adsorption.* Biomaterials, 2015. **52**: p. 531-538.
137. Melo, S.F., *Fibrous scaffolds of polymer/graphene oxide for antimicrobial biomedical applications*. 2012.
138. Wiegand, I., K. Hilpert, and R.E.W. Hancock, *Agar and broth dilution methods to determine the minimal inhibitory concentration (MIC) of antimicrobial substances.* Nature Protocols, 2008. **3**(2): p. 163-175.
139. Saporito, P., et al., *LL-37 fragments have antimicrobial activity against Staphylococcus epidermidis biofilms and wound healing potential in HaCaT cell line.* J Pept Sci, 2018. **24**(7): p. e3080.
140. Barbosa, M., et al., *Antimicrobial coatings prepared from Dhvar-5-click-grafted chitosan powders.* Acta Biomater, 2019. **84**: p. 242-256.
141. Nie, B.e., et al., *Covalent immobilization of KR-12 peptide onto a titanium surface for decreasing infection and promoting osteogenic differentiation.* RSC Advances, 2016. **6**(52): p. 46733-46743.
142. Pinto, A.M., et al., *Effect of incorporation of graphene oxide and graphene nanoplatelets on mechanical and gas permeability properties of poly(lactic acid) films.* Polymer International, 2013. **62**(1): p. 33-40.
143. Stobinski, L., et al., *Graphene oxide and reduced graphene oxide studied by the XRD, TEM and electron spectroscopy methods.* Journal of Electron Spectroscopy and Related Phenomena, 2014. **195**: p. 145-154.
144. Dreyer, D.R., et al., *The chemistry of graphene oxide.* Chem Soc Rev, 2010. **39**(1): p. 228-40.

145. Bykkam, S., et al., *Synthesis and characterization of graphene oxide and its antibacterial activity against Klebseilla and Staphylococus.* Int. J. Adv. Biotechnol. Res., 2013. **4**: p. 1005-1009.
146. Haynie, S.L., G.A. Crum, and B.A. Doele, *Antimicrobial activities of amphiphilic peptides covalently bonded to a water-insoluble resin.* Antimicrobial agents and chemotherapy, 1995. **39**(2): p. 301-307.
147. Cho, W.M., et al., *Design and synthesis of novel antibacterial peptide-resin conjugates.* Bioorg Med Chem Lett, 2007. **17**(21): p. 5772-6.